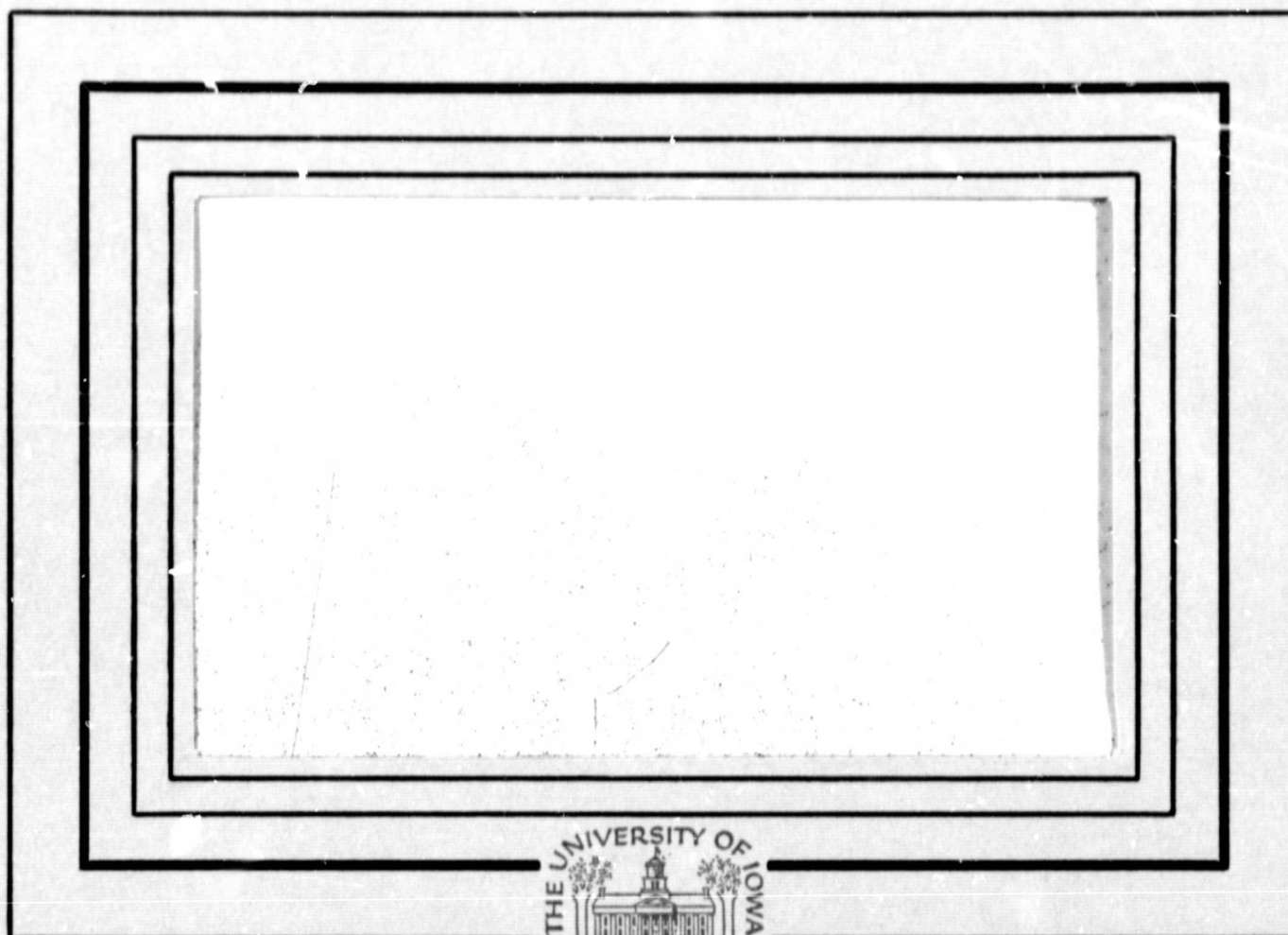


## **General Disclaimer**

### **One or more of the Following Statements may affect this Document**

- This document has been reproduced from the best copy furnished by the organizational source. It is being released in the interest of making available as much information as possible.
- This document may contain data, which exceeds the sheet parameters. It was furnished in this condition by the organizational source and is the best copy available.
- This document may contain tone-on-tone or color graphs, charts and/or pictures, which have been reproduced in black and white.
- This document is paginated as submitted by the original source.
- Portions of this document are not fully legible due to the historical nature of some of the material. However, it is the best reproduction available from the original submission.



Reproduction in whole or in part is permitted for any purpose of the United States Government.

Research was sponsored in part by the Office of Naval Research under contract N00014-68-A-0196-0003.

Department of Physics and Astronomy  
**THE UNIVERSITY OF IOWA**

Iowa City, Iowa

N 72-27835

G3/29

PAGE 69

Anisotropies in the Interplanetary Intensity  
of Solar Protons  $E_p > 0.3 \text{ MeV}^*$

by

WILLIAM G. INNANEN\*\*  
and  
JAMES A. VAN ALLEN

Department of Physics and Astronomy  
The University of Iowa  
Iowa City, Iowa 52240

June 1972

\* Research supported in part by the National Aeronautics and Space Administration under contract NAS5-9076 with Goddard Space Flight Center and by U. S. Office of Naval Research contract N00014-68-A-0196-0003.

\*\* NASA Pre-Doctoral Trainee 1965-1968.

DOCUMENT CONTROL DATA - R&D

(Security classification of title, body of abstract and indexing annotation must be entered when the overall report is classified)

1 ORIGINATING ACTIVITY (Corporate author) Department of Physics and Astronomy University of Iowa		2a REPORT SECURITY CLASSIFICATION UNCLASSIFIED	
		2b GROUP	
3 REPORT TITLE Anisotropies in the Interplanetary Intensity of Solar Protons $E_p > 0.3$ MeV			
4 DESCRIPTIVE NOTES (Type of report and inclusive dates) Progress, June 1972			
5 AUTHOR(S) (Last name, first name, initial) Innanen, William G., and Van Allen, James A.			
6. REPORT DATE June 1972		7a. TOTAL NO. OF PAGES 56	7b. NO. OF REFS 10
8a. CONTRACT OR GRANT NO. N00014-68-A-0196-0003		9a. ORIGINATOR'S REPORT NUMBER(S) U. of Iowa 72-15	
b. PROJECT NO.		9b. OTHER REPORT NO(S) (Any other numbers that may be assigned this report)	
c.			
d.			
10. AVAILABILITY/LIMITATION NOTICES Distribution of this document is unlimited.			
11. SUPPLEMENTARY NOTES		12. SPONSORING MILITARY ACTIVITY Office of Naval Research	
13. ABSTRACT  [See pages 2, 3, and 4 following]			

KEY WORDS	LINK A		LINK B		LINK C	
	ROLE	WT	ROLE	WT	ROLE	WT
Solar Protons						
Interplanetary Propagation						
Diffusive and Convective Transport						

#### INSTRUCTIONS

1. **ORIGINATING ACTIVITY:** Enter the name and address of the contractor, subcontractor, grantee, Department of Defense activity or other organization (*corporate author*) issuing the report.
- 2a. **REPORT SECURITY CLASSIFICATION:** Enter the overall security classification of the report. Indicate whether "Restricted Data" is included. Marking is to be in accordance with appropriate security regulations.
- 2b. **GROUP:** Automatic downgrading is specified in DoD Directive 5200.10 and Armed Forces Industrial Manual. Enter the group number. Also, when applicable, show that optional markings have been used for Group 3 and Group 4 as authorized.
3. **REPORT TITLE:** Enter the complete report title in all capital letters. Titles in all cases should be unclassified. If a meaningful title cannot be selected without classification, show title classification in all capitals in parenthesis immediately following the title.
4. **DESCRIPTIVE NOTES:** If appropriate, enter the type of report, e.g., interim, progress, summary, annual, or final. Give the inclusive dates when a specific reporting period is covered.
5. **AUTHOR(S):** Enter the name(s) of author(s) as shown on or in the report. Enter last name, first name, middle initial. If military, show rank and branch of service. The name of the principal author is an absolute minimum requirement.
6. **REPORT DATE:** Enter the date of the report as day, month, year; or month, year. If more than one date appears on the report, use date of publication.
- 7a. **TOTAL NUMBER OF PAGES:** The total page count should follow normal pagination procedures, i.e., enter the number of pages containing information.
- 7b. **NUMBER OF REFERENCES:** Enter the total number of references cited in the report.
- 8a. **CONTRACT OR GRANT NUMBER:** If appropriate, enter the applicable number of the contract or grant under which the report was written.
- 8b, 8c, & 8d. **PROJECT NUMBER:** Enter the appropriate military department identification, such as project number, subproject number, system numbers, task number, etc.
- 9a. **ORIGINATOR'S REPORT NUMBER(S):** Enter the official report number by which the document will be identified and controlled by the originating activity. This number must be unique to this report.
- 9b. **OTHER REPORT NUMBER(S):** If the report has been assigned any other report numbers (*either by the originator or by the sponsor*), also enter this number(s).
10. **AVAILABILITY/LIMITATION NOTICES:** Enter any limitations on further dissemination of the report, other than those

imposed by security classification, using standard statements such as:

- (1) "Qualified requesters may obtain copies of this report from DDC."
- (2) "Foreign announcement and dissemination of this report by DDC is not authorized."
- (3) "U. S. Government agencies may obtain copies of this report directly from DDC. Other qualified DDC users shall request through \_\_\_\_\_."
- (4) "U. S. military agencies may obtain copies of this report directly from DDC. Other qualified users shall request through \_\_\_\_\_."
- (5) "All distribution of this report is controlled. Qualified DDC users shall request through \_\_\_\_\_."

If the report has been furnished to the Office of Technical Services, Department of Commerce, for sale to the public, indicate this fact and enter the price, if known.

11. **SUPPLEMENTARY NOTES:** Use for additional explanatory notes.

12. **SPONSORING MILITARY ACTIVITY:** Enter the name of the departmental project office or laboratory sponsoring (*paying for*) the research and development. Include address.

13. **ABSTRACT:** Enter an abstract giving a brief and factual summary of the document indicative of the report, even though it may also appear elsewhere in the body of the technical report. If additional space is required, a continuation sheet shall be attached.

It is highly desirable that the abstract of classified reports be unclassified. Each paragraph of the abstract shall end with an indication of the military security classification of the information in the paragraph, represented as (TS), (S), (C), or (U).

There is no limitation on the length of the abstract. However, the suggested length is from 150 to 225 words.

14. **KEY WORDS:** Key words are technically meaningful terms or short phrases that characterize a report and may be used as index entries for cataloging the report. Key words must be selected so that no security classification is required. Identifiers, such as equipment model designation, trade name, military project code name, geographic location, may be used as key words but will be followed by an indication of technical context. The assignment of links, roles, and weights is optional.

## ABSTRACT

From a much larger body of data on solar protons  $E_p > 0.3$  MeV obtained by Explorer 35 since July 1967, the following ten events were selected for the detailed study of intensity vs time and of angular distributions of intensity in interplanetary space near the earth: November 18, 1968; August 9, 1967; May 13, 1969; January 24, 1969; March 21, 1969; June 25, 1970; January 31, 1970; July 1, 1970; November 27, 1967; and July 6, 1970. The bases of selection were that the events be of adequate intensity for statistically satisfactory study and that they be "simple"--that is, reasonably attributable to a single solar flare so that their time histories were not complicated by overlapping emissions of particles. The principal findings for these events are as follows:

(a) The time-integrated value of the net anti-solar flux of protons  $E_p > 0.3$  MeV over these several events ranged from  $10^{33}$  to  $10^{35}$  protons per steradian, the result being expressed as the number of particles per unit solid angle at 1 AU referenced to the sun as the apex of the infinitesimal solid angle. The events caused by flares near the central meridian of the sun

usually produced the greatest values of time-integrated outward flux though the general significance of this result is limited since the ten selected events may not constitute a representative sample of solar events.

(b) An anisotropy vector ( $C, \delta$ ) in the ecliptic plane has been calculated as a function of time from the detailed angular distribution data. Following earlier work on much more energetic solar protons  $7.5 < E_p < 45$  MeV by McCracken et al. [1968, 1971] and theoretical guidance by Forman [1970a, 1970b] the observed anisotropy vector was resolved into two components: one radial from the sun,  $C_R$ , and one along the local magnetic field line,  $C_M$ . These components are given as a function of time.

(c) During the early phases of the events,  $C_M$  is the dominant component of the anisotropy. Later, during the decay phases, the anisotropy vector is only weakly correlated with the magnetic field direction.

(d) Throughout most of the events (one significant exception), the radial component of the anisotropy is uniformly positive (outward from the sun) and of magnitude in good agreement with theoretical values of the convective anisotropy calculated from observed values of solar wind velocity and spectral indices.

(e) The decay phase value of the field aligned component of the anisotropy vector, assumed to be diffusive in nature, is negative in many cases, and yields a value of  $K \cdot \nabla U / U$  as great

as  $7 \times 10^{20} \text{ cm}^2/\text{sec} - \text{AU}$ , where  $K$  is the diffusion tensor and  $U$  is the particle density. In other cases the anisotropy during this period is slightly positive or indistinguishable from zero.

(f) The field aligned component of the anisotropy in the rising phase of some events diminishes over a period of a day or two down to the decay phase values. A typical peak magnitude of this component, if interpreted as being caused by diffusive transport of protons, yields a value of  $K \cdot \nabla U / U$  of  $-3 \times 10^{21} \text{ cm}^2/\text{sec} - \text{AU}$ .

(g) The fact that strong field aligned proton anisotropies are observed for events produced by eastern flares indicates that interior to the earth's orbit the particle distribution has been spread over a broad range of solar longitude.



## INTRODUCTION

The frequent solar emission of protons in the energy range down to and below 1 MeV was first established in 1961 by measurements on Injun 1 [Pieper et al., 1962] and in 1962 by measurements on Mariner 2 [Van Allen and Frank, 1962] [Van Allen et al., 1964]. Such events have now been monitored on a nearly continuous basis over a full solar activity cycle of 11 years by University of Iowa equipment on a series of earth satellites and space probes. The most comprehensive measurements in the sub-MeV energy range over an extended period of time have been conducted by Explorer 33 from July 1, 1966 to November 1, 1971 and by Explorer 35 beginning on July 19, 1967 and continuing at the present date. A technique for measuring the angular distribution of the intensity of protons  $E_p > 0.3$  MeV in interplanetary space was first introduced on Explorer 33, whose spin axis was approximately in the ecliptic plane. The same technique was applied to Explorer 35, with more valuable results because of the more favorable orientation of the spin axis.

The present paper gives the first detailed studies of the angular distributions of solar proton intensities in interplanetary space in the low energy range  $E_p \geq 0.3$  MeV. Solar proton intensity

data from two channels of the University of Iowa solid state detector on Explorer 35 [Van Allen and Ness, 1969] are used for this purpose. Explorer 35 has been in lunar orbit since July 22, 1967. The spacecraft has an eccentric orbit with a period of approximately 11.5 hours and spins about an axis which is oriented to within  $7^\circ$  of the perpendicular to the ecliptic plane. The solid state detector has its axis perpendicular to the spin axis so that it sweeps around the ecliptic plane with the spin period of about 2.5 seconds. The single element detector has four channels: P1, which is sensitive primarily to protons with energies 0.322 to 6.3 MeV; P2, sensitive to protons with energies 0.478 to 3.0 MeV; P3, which is sensitive only to particles of  $Z \geq 3$ ; and P4, which is sensitive primarily to alpha particles in the energy range 2.0 to 10.2 MeV.

Counts from the channels of interest here, P1 and P2, are accumulated in a spin averaged mode. In addition, counts from the P1 channel are divided into four equal sectors in the ecliptic plane. The longitude ranges of the detector's axis in spacecraft centered solar ecliptic coordinates during accumulation of counts in the respective sectors are as follows: Sector I,  $230^\circ$  to  $140^\circ$ ; Sector II,  $140^\circ$  to  $50^\circ$ ; Sector III,  $50^\circ$  through  $0^\circ$  to  $320^\circ$ ; and Sector IV,  $320^\circ$  to  $230^\circ$ . During optical eclipse by the moon the sectoring is maintained by an artificial "see-sun" pulse. However, due to thermal shrinkage in the spacecraft and a consequent spin-

up, there is a progressive slippage of the sector pattern relative to the spacecraft-sun line. Data from these periods have been excluded because of the tedium of the correction procedure.

All channels of the solid state detector have an inverse unidirectional geometric factor of  $12.7 \text{ (cm}^2 \text{ sr)}^{-1}$ . There is an onboard radioactive alpha particle source that gives continuous background counting rates to assure the proper operation of the detector. These background counting rates have been subtracted prior to all calculations. The P1 and P2 background counting rates are, respectively, 0.0705 and 0.0506 counts/second.

At perihelion the moon blocks a significant portion of the detector's field of view, thus reducing the proton flux from that direction [Van Allen and Ness, 1969]. In averages, however, and especially in averages of several hours or more, the moon, due to its rapid angular motion relative to the spacecraft, blocks a particular portion of the sectoring diagram for only a fraction of the averaging period, thus reducing its effect on the directional information of the solar protons to a small value, which is barely significant in the data presented in this work. In half hour data there are occasional periods of otherwise very steady counting rates when lunar shadowing causes an observable modulation.

For the study of solar protons in the interplanetary medium, the data are assumed free of magnetospheric effects when the

spacecraft is located outside of the average magnetosheath location as observed and reported by Behannon [1968].

One-half hour averages of the counting rates of the proton detector channels are used as the base of all data analysis in this paper.

## DATA ANALYSIS

A least squares fit to the half-hour counting rates of the four directional sectors of channel P1 is made to an anisotropy model with a unidirectional particle flux of the form:

$$j(\varphi) = A [1 - C \cos(\varphi - \delta)], \quad (1)$$

where A is the spin averaged value of j; C is the magnitude of the anisotropy;  $\varphi$  is the longitude of the detector's axis in spacecraft centered solar ecliptic coordinates;  $\delta$  is equal to  $\varphi_{\max} + 180^\circ$  or  $\varphi_{\max} - 180^\circ$ , whichever is positive and less than  $360^\circ$ ; and  $\varphi_{\max}$  is the value of  $\varphi$  for which j is a maximum. The angles  $\varphi$  and  $\delta$  are measured from the spacecraft-sun line in the counter-clockwise sense as viewed from the north ecliptic pole.  $\varphi_{\max}$  specifies the direction in which the detector is looking at maximum counting rate;  $\delta$  specifies the spacecraft centered longitude toward which the maximum particle intensity is directed. Note that

$$C = \frac{j_{\max} - j_{\min}}{j_{\max} + j_{\min}}.$$

For each set of parameters, the observed anisotropy vector is defined as the vector  $(C, \delta)$ . It is, of course, only the projection on the ecliptic plane of the full, three-dimensional anisotropy vector.

An exemplary case of actual data for the half-hour period 0130-0200 UT of August 11, 1967 is as follows:

Sector I	226.8 counts/sec
Sector II	220.5
Sector III	441.1
Sector IV	427.2

From these data:

$$\begin{aligned}
 A &= 328.8 \text{ counts/sec} = 4176 \text{ (cm}^2 \text{ sec sr)}^{-1} \\
 C &= 0.503 \\
 \varphi_{\max} &= 320^\circ \\
 \delta &= 140^\circ
 \end{aligned}$$

The limitations of equation (1) are recognized but the nature of the basic angular distribution data does not appear to justify a more elaborate analysis.

Anisotropy vectors for periods of greater than a half-hour are found by taking the separate means of the two cartesian components of each of the half hour vectors included. The result is then re-expressed as a polar vector.

Since P1 and P2 detect protons over different energy ranges, the ratio P1/P2 gives information on the form of the proton energy distribution. Inasmuch as the relevant spectral quantity in the present investigation is the logarithmic derivative

$$\frac{d [\ln (\frac{dj}{dE})]}{d [\ln E]},$$

where E is kinetic energy, a power law differential spectrum of the simple form

$$\frac{dj}{dE} = K E^{\gamma} \quad (2)$$

has been adopted as adequate over the limited energy range of importance (0.3 to several MeV). Because the energy ranges of P1 and P2 are nested, there are in general two possible values of  $\gamma$  corresponding to a given P1/P2 ratio, one greater than -1.39 and one less than -1.39. Conclusive resolution of this ambiguity has been accomplished in a number of cases by use of simultaneous polar cap data from the earth-orbiting satellite Injun 5. (See later section.)

Two different graphical representations of the anisotropy data are used in this study. The first is a direct plot of the anisotropy and spectral parameters A, C,  $\delta$ , and  $\gamma$  versus time [Figures 8-14]. The error bars on all quantities are omitted when they are of the order of the point size. When the counting rates are low, or when both values of  $\gamma$  are approximately -1.39, the calculated uncertainty in the ratio P1/P2 may show that the

uncertainties in both values are larger than the difference between the two values. Then both points are shown on a single combined error bar. Along the top border of the plots there are several symbols which indicate the location of the spacecraft. The triangles indicate the times of periapse, a solid line indicates that the spacecraft is within the average boundaries of the magnetotail, and a dashed line indicates that the spacecraft is outside of the magnetotail but behind the average location of the earth's bow shock [Behannon, 1968].

The second useful representation of the proton anisotropy data is the "anisotropy vector sum" plot. Such a plot is produced by arranging successive anisotropy vectors "head to tail" to show the time dependence of the anisotropy vector [Figures 1-7]. In the plots given here, the anisotropy vectors are six hour averages. Also the average orientation (i.e., ignoring the vector sense) of the interplanetary magnetic field is shown for each anisotropy vector by a light line through its tail. Alpha is the angle between the anisotropy vector and the magnetic field line.

Other data used in this paper include one-hour magnetic field averages from Explorer 35 kindly supplied by K. W. Behannon and N. F. Ness of the Goddard Space Flight Center and by D. S. Colburn of the Ames Research Center. The solar wind data are from the Vela satellites of the Los Alamos Scientific Laboratory as published



in Solar Geophysical Data 1969 through 1970. During the years 1969 and 1970 the maximum reported solar wind velocity was 770 km/sec on January 26, 1969 and the minimum was 234 km/sec on June 23, 1970.

NET FLUX OF PROTONS  $E_p > 0.3$  MeV

Using the parameters A, C, and  $\delta$  from the fitting of equation (1) to observed data, the net flux of protons, f, through a unit area perpendicular to the spacecraft-sun line is given by

$$f = 12.7 \int_0^{2\pi} A [1 - C \cos(\varphi - \delta)] \cos \varphi d\varphi$$

or

$$f = -12.7 \pi A C \cos \delta . \quad (3)$$

The quantity f is positive (net flux outward from the sun) for  $90^\circ < \delta < 270^\circ$  and negative (net flux inward toward the sun) for  $0^\circ < \delta < 90^\circ$  and  $270^\circ < \delta < 360^\circ$ . It is conveniently measured in  $(\text{cm}^2 \text{ sec})^{-1}$ . The time integral of f over a particular solar particle event gives the total number of particles per unit area flowing past the spacecraft for that event. The result has been expressed as the number of particles per unit solid angle at 1 AU referenced to the sun as the apex of the infinitesimal solid angle. No

implications of rectilinear propagation or of isotropic emission at the sun are intended by this convention.

Table 1 gives  $N$ , the number of protons  $E_p > 0.3$  MeV per steradian flowing past the spacecraft during the course of the event, for those "simple" events under study by observations essentially clear of the magnetosphere. "Simple" events are those whose time history suggests that they are attributable to a single solar flare. They are characterized, generally, by a rise phase of 1 to 2 days duration and a decay phase of 3 to 8 days duration. The intensity-time curves are grossly, but not accurately, monotonic during the respective phases.

Solar particle events are identified with particular flares by comparing the onset times of high energy protons, prompt energetic electrons, and solar X rays (all of which are available from the University of Iowa experiment on Explorer 35) to the onset time of optical flares as tabulated in Solar-Geophysical Data of the U. S. Department of Commerce. Usually one flare can be identified with reasonable certainty as being the parent flare for an event. An exception is the event of May 13, 1969 which had a very gradual onset in both high energy protons and energetic electrons, and no discernible X-ray emission. The only flares occurring near the presumed time of particle emission were sub-flares. Thus it appears reasonably certain that this event must be attributed to a flare on the invisible hemisphere of the sun.

Several conclusions can be drawn from the information in Table 1. First there is a clear positive correlation between the maximum intensity of an event and  $N$ . This non-surprising result simply means that the form of intensity-time curves is more or less independent of the "size" of the event. Table 2 shows the average value of  $N$  for three ranges of maximum intensity in the events. Because the number of events clear of the magnetosphere is small, the results in Table 2 can not be taken, however, as thoroughly definitive.

Another observation from Table 1 concerns the relationship of  $N$  to the solar longitude of the parent flare. If the dominant mode of transport for 0.3 MeV solar protons were convective with little or no diffusion either along or across the interplanetary magnetic field lines, one would expect the flare longitudes to be clustered around  $0^\circ$ . If the dominant transport mechanism were fast diffusion along field lines, with little or no convection and slow cross field diffusion (the case for higher energy protons), then one would expect to find the largest events from flares around west  $50^\circ$  solar longitude (where the interplanetary magnetic field lines through the earth reach the sun). Mixing the convective and parallel field diffusive transport mechanisms would give an optimal flare longitude between these extremes. An increasingly important degree of cross field diffusion would tend to smear this distribution.

Despite the small number of events in Table 1, and the statistical inadequacy of the body of data, it is of interest that the events with the largest N values are clustered around or somewhat to the east of  $0^\circ$  solar longitude. The one exception to this is the November 18, 1968 event, which was caused by a western limb flare, and which, judging from the particle data, was by far the largest simple event of those under study. If a similar clustering around  $0^\circ$  solar longitude were observed for an adequately large number of events, this evidence alone would suggest radial convection as the dominant transport mechanism for protons  $E_p \gtrsim 0.3$  MeV.

# THE DIFFUSIVE AND CONVECTIVE COMPONENTS OF THE ANISOTROPY

Figures 1 through 7 show anisotropy vector sum plots for the seven largest events of those being studied. The vectors are six hour averages in all cases. Figures 8 through 14 show the  $A$ ,  $C$ ,  $\delta$ , and  $\gamma$  versus time plots for the same seven events. Several common characteristics are seen in these data. During the rise phase of each event the anisotropy vector tends to align itself with the interplanetary magnetic field more closely than it does later in the event. During the rise phases of all but the June 25, 1970 event (Figure 7)  $\alpha$ , the angle between the field line and the anisotropy vector, tends to be negative, that is, the anisotropy vector, while being nearly in the same direction as the interplanetary field lines, lies between the field line orientation and the outward radial direction. During the decay phases the anisotropy tends to be more nearly radially outward and less dependent on the field direction. These observations are in qualitative agreement with those by McCracken et al. [1968] for 7.5 to 45 MeV solar protons.

The above results support the hypotheses (a) that in the early portion of a solar proton event the dominant particle,

transport mechanism is diffusive, with the diffusion tensor such that diffusion takes place primarily along the magnetic field lines and (b) that later in the event the anisotropy is mainly attributable to radially outward convection by the solar wind.

The matter has been discussed in convenient theoretical form by Forman [1970a] [1970b]. There she divides the theoretical anisotropy vector  $\Delta$  into two components:  $\Delta_d$ , the diffusive component, and  $\Delta_c$ , the convective component. The diffusive component of the anisotropy vector is determined by the gradient in the particle density  $U$  and the diffusion tensor  $K$ :

$$\Delta_d = - \frac{3}{v} \cdot \frac{K \cdot \nabla U}{U} \quad (4)$$

where  $v$  is the particle velocity. The convective component is the kinematic anisotropy which results from transforming any assumed distribution in the rest frame of the solar wind to the observer's frame of reference (Compton-Getting effect). For an infinitesimal portion of a continuous particle spectrum at kinetic energy  $E$  and velocity  $v$  the theoretical value of the convective component of the anisotropy vector is

$$\Delta_c = \left\{ 2 - \alpha \frac{d [\ln (\frac{dj}{dE})]}{d [\ln E]} \right\} \frac{v}{v} \quad (5)$$

where  $V$  is the convection or solar wind velocity,  $\alpha = 2$  for 0.3 MeV protons, and  $dj/dE$  is the differential energy spectrum of the particles at energy  $E$ . For the adopted spectral form of equation (2), equation (5) becomes:

$$\Delta_c = (2 - 2\gamma) V \left\langle \frac{1}{v} \right\rangle \quad (6)$$

where  $\left\langle \frac{1}{v} \right\rangle$  is the spectral average of the reciprocal particle velocity over the energy range of the detector. Assuming that  $K$  is such that diffusion along the field predominates over cross field diffusion,  $\Delta_d$  will be along the field line and  $\Delta_c$  will be radially outward.

In view of the above theoretical guidance the observed anisotropy vector  $(C, \delta)$  is resolved into two components: a radial component with magnitude  $C_R$ , and a field aligned component with magnitude  $C_M$  (see Figure 15). The magnitude of the components is considered positive outward from the sun. The identification of  $C_R$  with  $\Delta_c$  and  $C_M$  with the diffusive anisotropy  $\Delta_c$  is valid only insofar as field aligned diffusion dominates cross field diffusion.

Figures 16 through 22 show  $C_M$  and  $C_R$  for the seven above mentioned events. The values are six hour averages of one hour  $C_R$  and  $C_M$  data. The error bars show the statistical standard deviations of the one hour data from the mean value during the six hour period. In periods of low counting rate, because of poor



statistics, sometimes not all six values are included in the average, thus causing the standard deviation to possibly be an underestimation of the scatter. When the interplanetary magnetic field approaches the radial direction, the resolution of the anisotropy vector into  $C_R$  and  $C_m$  becomes indeterminate. Thus, in cases when the field is within  $10^\circ$  of the radial direction, resolution of the anisotropy vector has not been attempted.

The significance of  $C_R$  is examined with the help of equation (6) for the theoretical value of  $\Delta_c$ , the convective component of the anisotropy. As remarked earlier and as shown explicitly in Figures 8-14, two different values of the spectral parameter  $\gamma$  are found, in general, for any observed ratio  $P1/P2$ . Hence, two, usually quite different, values of  $\Delta_c$  are found by equation (6).

To resolve this ambiguity a comparison of Explorer 35 spectral data was made with spectral data in a similar energy range obtained from simultaneous observations of solar protons over the polar caps of the earth with the University of Iowa satellite Injun 5. An unambiguous value for  $\gamma$  was obtained from the ratio of the counting rates of the  $0.3 \leq E_p \leq 9.2$  MeV channel to the  $0.3 \leq E_p \leq 1.4$  MeV channel of the solid state detector of Injun 5. This comparison was possible for the following periods of those under study: decimal days 24.0 to 26.0, 1969; days

80.0 to 85.0, 1969; days 134.0 to 136.0, 1969; and days 32.0 to 34.0 1970 (decimal day 0.5 being 1200 UT January 1). In these four cases, all of some 36 Injun 5 values of  $\gamma$ , without exception, were accurately consistent with the  $\gamma < -1.39$  branch of the ambiguous Explorer 35 curve of P1/P2 vs  $\gamma$  and were clearly inconsistent with the  $\gamma > -1.39$  branch. On the basis of this evidence for four specific events, it is concluded tentatively that the more negative value of  $\gamma$  is the proper choice for all of the events under study here.

Hence, a unique value of  $\Delta_c$  is found by equation (6), using Vela values of  $V$  whenever such data are available. These theoretical values of  $\Delta_c$  are shown as open squares in Figures 18-22 for comparison with the observed values of  $C_R$ .

In the decay phases of all events for which this comparison has been possible, there is excellent agreement between  $\Delta_c$  and  $C_R$ , thus supporting the hypothesis that the radial component of the anisotropy in the decay phase of a solar proton event is attributable to the convection of protons by frozen-in magnetic irregularities in the solar wind.

Further, during the rise phase of most events,  $C_R$  behaves in a corresponding manner; that is, it is positive and relatively constant in magnitude at a value consistent with usual values of  $V$ , even though observed values of  $V$  are somewhat sparse. An exception seems to be the rise phase of the event of June 25, 1970 (Figure 22).

Here  $C_M$  is strongly positive early in the event. At corresponding times  $C_R$  is strongly negative; later  $C_R$  becomes zero then goes positive and remains approximately constant at  $\sim 0.4$  during the decay phase as  $C_M$  tends toward zero and then toward negative values. No explanation for this case is offered, though it is clear also from Figure 7 that this is an unusual event.

Insofar as the above evidence justifies the identification of  $C_R$  with the theoretical convective anisotropy  $\Delta_c$  in the decay phase of simple solar events, and, in some cases, also in the rise phase, then, by elimination,  $C_M$  must be the diffusive contribution to the anisotropy during these periods. Making this identification, we can draw some inferences about the particle density gradient using equation (4).

For the events of November 18, 1968 (Figure 17), March 21, 1969 (Figure 19), January 31, 1970 (Figure 21), and June 25, 1970 (Figure 22)  $C_M$  is negative for a significant portion, if not most, of the decay phase. This is taken to mean that there is a positive radial gradient in the particle density  $U$  (i.e.,  $U$  increases with increasing heliocentric distance), thus causing a sunward diffusion of protons. Since the particles were injected initially at the sun, it appears that the positive gradient must have been caused by the bulk convective transport of particles outward by the solar wind [cf. McCracken et al., 1971]. This observation gives striking evidence for the importance of convection at these energies.

A typical value of  $C_M$  during these positive gradient periods is about -0.2, which gives, by equation (4), a value for  $K \cdot \nabla U/U$  of about  $7 \times 10^{20} \text{ cm}^2/\text{sec} - \text{AU}$ .

In those rise phase cases where  $C_R$  can be identified with the theoretical convective anisotropy, such as in the August 9, 1967 event (Figure 16) and the March 21, 1969 event (Figure 19), the behavior of  $C_M$  is qualitatively what one would expect of the diffusive component of the anisotropy, namely,  $C_M$  decays from a high positive initial value to the decay phase values over a period of one or two days. A typical initial rise phase value for  $C_M$  of +1.0 corresponds to a negative radial gradient in the particle density with  $K \cdot \nabla U/U$  of about  $-3 \times 10^{21} \text{ cm}^2/\text{sec} - \text{AU}$ . Since both of these cases are from eastern flares, the fact that protons are diffusing down magnetic field lines near the earth that lead to the western side of the sun indicates that protons  $E_p \gtrsim 0.3 \text{ MeV}$  are injected into, or diffuse into, a region interior to the earth's orbit that is very broad in solar longitude.

McCracken et al. [1968] have reported the effects of interplanetary magnetic field reversals on 7.5 MeV solar protons. The observed effects on 0.3 MeV solar protons for the periods under study here are variable. During the March 21, 1969 event there is a single magnetic field reversal (Figure 4) which, while having observable effects on A, C, and  $\delta$  (Figure 11), had no effect on  $C_R$  and did not interrupt the decay of  $C_M$  (Figure 19).

In the May 13, 1969 event there was a series of field reversals and irregularities. In this event  $C_M$  (Figure 20) remained positive and relatively constant indicating that protons were diffusing outward from the sun for the entire event despite the field reversals. In the January 31, 1970 event there were many interplanetary magnetic field irregularities. As seen in Figure 21,  $C_M$  in the decay phase of this event was negative, indicating diffusion inward along the field lines toward the sun.

## ACKNOWLEDGEMENTS

This paper is based on the Ph.D. dissertation of the first author [Innanen, 1972], wherein a considerably larger body of data and additional details are given. The solid state detector on the NASA/GSFC satellite Explorer 35 was developed at the University of Iowa by Drs. S. M. Krimigis and T. P. Armstrong. Interplanetary magnetic field data from the two magnetometers on Explorer 35 were kindly supplied by Drs. K. W. Behannon and N. F. Ness of the Goddard Space Flight Center and Dr. D. S. Colburn of the Ames Research Center. The data on the solar wind velocities were taken from Los Alamos Scientific Laboratory observations with the Vela satellites as published in Solar-Geophysical Data of the U. S. Department of Commerce.

One of us (W.G.I.) is grateful for a NASA predoctoral traineeship 1965-68.

The hardware phase of this work was supported by contract NAS5-9076 with the Goddard Space Flight Center. Analytical work has been supported by contract N00014-68-A-0196-0003 with the U. S. Office of Naval Research.

## REFERENCES

- Behannon, K. W., Mapping of the earth's bow shock and magnetic tail by Explorer 33, J. Geophys. Res., 73, 907-930, 1968.
- Forman, M. A., The Compton-Getting effect for cosmic-ray particles and photons and the Lorentz-invariance of distribution functions, Planet. Space Sci., 18, 25-31, 1970a.
- Forman, M. A., The equilibrium anisotropy in the flux of 10-MeV solar particles and their convection in the solar wind, J. Geophys. Res., 75, 3147-3153, 1970b.
- Innanen, W. G., Anisotropies in 0.3 MeV solar protons, Ph.D. dissertation, University of Iowa, May 1972.
- McCracken, K. C., U. R. Rao, R. P. Bukata, and E. P. Keath, The decay phase of solar flare events, Solar Phys., 18, 100-132, 1971.
- McCracken, K. C., U. R. Rao, and N. F. Ness, Interrelationship of cosmic-ray anisotropies and the interplanetary magnetic field, J. Geophys. Res., 73, 4159-4166, 1968.
- Pieper, G. F., A. J. Zmuda, C. O. Bostrom, and B. J. O'Brien, Solar protons and magnetic storms in July 1961, J. Geophys. Res., 67, 4959-4981, 1962.

Van Allen, J. A., and L. A. Frank, Mariner II. The Iowa radiation experiment, Science, 138, 1097-1098, 1962.

Van Allen, J. A., L. A. Frank, and D. Venkatesan, Trans., Am. Geophys. Union, 45, 80, 1964 (Abstract P27).

Van Allen, J. A., and N. F. Ness, Particle shadowing by the moon, J. Geophys. Res., 74, 71-93, 1969.



Table 1

A Table of N for Simple Events Clear of the Magnetosphere  
(See Text)

Event of	Decimal Days From	Days To	N (protons/sr)	Maximum Intensity (c/s)	Flare Longitude	Flare Importance
Nov. 18, 1968	322.50	333.00	$1.6 \times 10^{35}$	$1.8 \times 10^3$	W 70°	** 1B
Aug. 9, 1967	220.75	226.00	$9.8 \times 10^{34}$	$5.3 \times 10^2$	E 32°	2B
May 13, 1969	132.75	140.00	$9.4 \times 10^{34}$	$1.3 \times 10^3$	***	***
Jan. 24, 1969	23.33	30.00	$8.6 \times 10^{34}$	$2.2 \times 10^2$	W 09°	2B
Mar. 21, 1969	79.00	88.00	$5.5 \times 10^{34}$	$3.0 \times 10^2$	E 16°	2N
June 25, 1970	175.50	181.00	$4.3 \times 10^{34}$	$9.2 \times 10^2$	E 11°	2B
Jan. 31, 1970	30.75	36.00	$1.6 \times 10^{34}$	$1.9 \times 10^2$	W 62°	2B
July 1, 1970	181.00	186.75	$9.8 \times 10^{33}$	$1.0 \times 10^2$	E 83°	1F
Nov. 27, 1967	330.00	336.25	$5.9 \times 10^{33}$	$7.0 \times 10^1$	W 41°	1F
July 6, 1970	186.75	192.00	$5.1 \times 10^{33}$	$2.5 \times 10^1$	W 90°	1B**

\*\* West limb flare

\*\*\* Subflares only

Table 2

A Table of N for Several Ranges of Maximum Intensity  
for Simple Events Clear of the Magnetosphere

Maximum Intensity Range (c/s)	Average N (protons/sr)	Number of Events
$I > 9 \times 10^2$	$9.8 \times 10^{34}$	3
$10^2 < I < 9 \times 10^2$	$3.9 \times 10^{34}$	5
$10^1 < I < 10^2$	$5.5 \times 10^{33}$	2

## FIGURE CAPTIONS

- Figure 1. Anisotropy vector sum plot (six-hour averages) for the event of August 9, 1967. The  $X_{SE}$   $Y_{SE}$   $Z_{SE}$  coordinate system is a spacecraft centered one with the  $X_{SE}$   $Y_{SE}$  plane parallel to the ecliptic, the  $+X_{SE}$  axis toward the sun, and the  $+Z_{SE}$  axis toward the north ecliptic pole.
- Figure 2. Anisotropy vector sum plot (six-hour averages) for the event of November 18, 1968.
- Figure 3. Anisotropy vector sum plot (six-hour averages) for the event of January 24, 1969.
- Figure 4. Anisotropy vector sum plot (six-hour averages) for the event of March 21, 1969.
- Figure 5. Anisotropy vector sum plot (six-hour averages) for the event of May 13, 1969.
- Figure 6. Anisotropy vector sum plot (six-hour averages) for the event of January 31, 1970.
- Figure 7. Anisotropy vector sum plot (six-hour averages) for the event of June 25, 1970.
- Figure 8. Anisotropy parameters and indices of a power law energy spectrum (see text) for the period decimal days 220.0 through 226.0, 1967 (decimal day 220.0 =

August 9 on 0000 UT). The parent flare occurred on decimal day 220 at 1815 UT.

Figure 9. Anisotropy parameters and indices of a power law energy spectrum (see text) for the period decimal days 322.0 through 333.0, 1968 (decimal day 322.0 = November 18 at 0000 UT). The parent flare occurred on decimal day 322 at 1017 UT.

Figure 10. Anisotropy parameters and indices of a power law energy spectrum (see text) for the period decimal days 23.0 through 31.0, 1969 (decimal day 23.0 = January 24 at 0000 UT). The parent flare occurred on decimal day 23 at 0803 UT.

Figure 11. Anisotropy parameters and indices of a power law energy spectrum (see text) for the period decimal days 79.0 through 88.0, 1969 (decimal day 79.0 = March 21 at 0000 UT). The parent flare occurred on decimal day 79 at 0141 UT.

Figure 12. Anisotropy parameters and indices of a power law energy spectrum (see text) for the period decimal days 132.0 through 140.0, 1969 (decimal day 132.0 = May 13 at 0000 UT). No major flares preceded the onset of the event.

Figure 13. Anisotropy parameters and indices of a power law energy spectrum (see text) for the period decimal days 30.0 through 36.0, 1970 (decimal day 30.0 = January 31 at 0000 UT). The parent flare occurred on decimal day 30 at 1512 UT.

Figure 14. Anisotropy parameters and indices of a power law energy spectrum (see text) for the period decimal days 175.0 through 181.0, 1970 (decimal day 175.0 = June 25 at 0000 UT). The parent flare occurred on decimal day 175 at 1833 UT.

Figure 15. An illustration of the resolution of the observed anisotropy vector  $C$  into a radial component  $C_R$  and a component  $C_M$  along the local magnetic field line  $BB'$ . The diagram is in the ecliptic plane. The sense of the magnetic vector is ignored.

Figure 16. The anisotropy components  $C_M$  and  $C_R$  for the event of August 9, 1967.

Figure 17. The anisotropy components  $C_M$  and  $C_R$  for the event of November 18, 1968.

Figure 18. The anisotropy components  $C_M$  and  $C_R$  for the event of January 24, 1969. The open squares are calculated values of  $\Delta_c$ .

Figure 19. The anisotropy components  $C_M$  and  $C_R$  for the event of March 21, 1969. The open squares are calculated values of  $\Delta_c$ .

Figure 20. The anisotropy components  $C_M$  and  $C_R$  for the event of May 13, 1969. The open squares are calculated values of  $\Delta_c$ .

Figure 21. The anisotropy components  $C_M$  and  $C_R$  for the event of January 31, 1970. The open squares are calculated values of  $\Delta_c$ .

Figure 22. The anisotropy components  $C_M$  and  $C_R$  for the event of June 25, 1970. The open squares are calculated values of  $\Delta_c$ .

AUGUST 9, 1967 EVENT

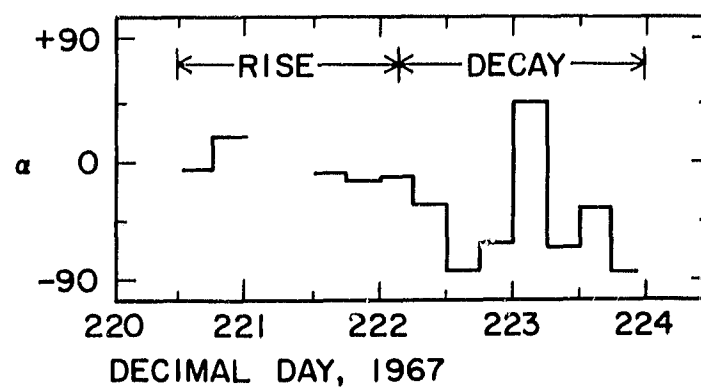
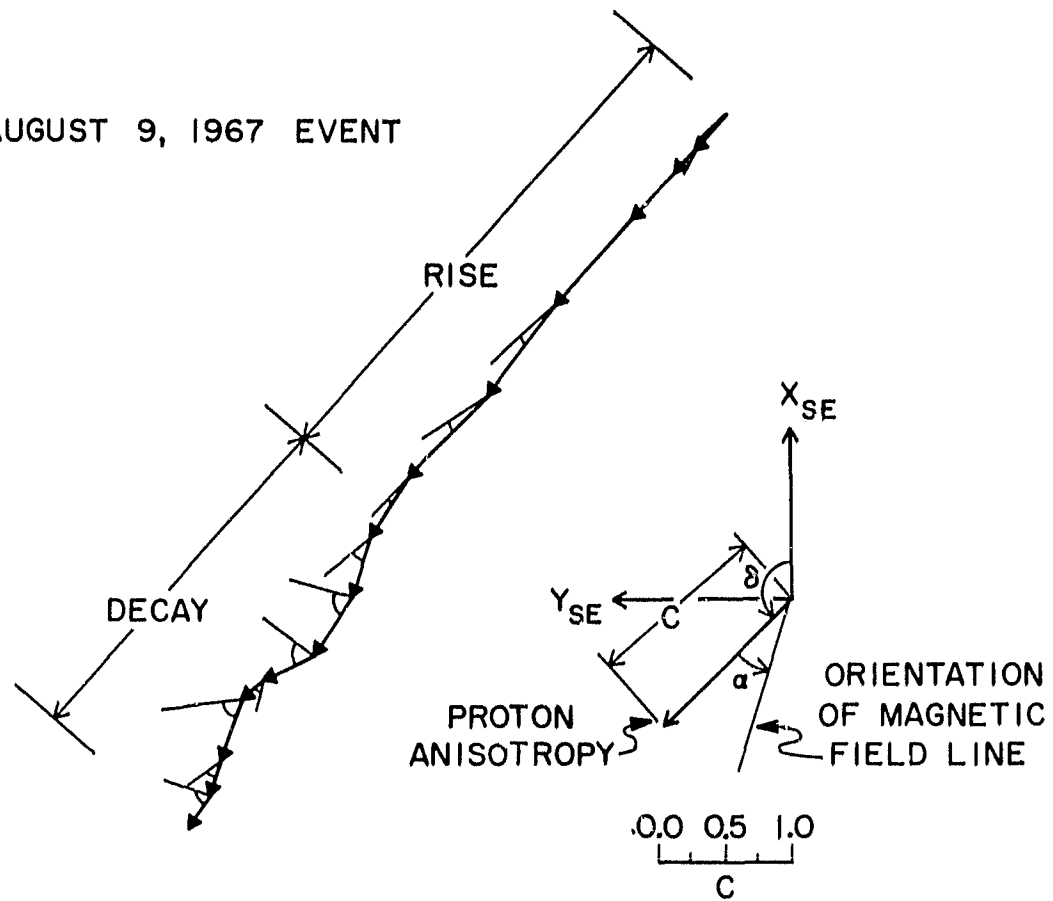


Figure 1

NOVEMBER 18, 1968 EVENT

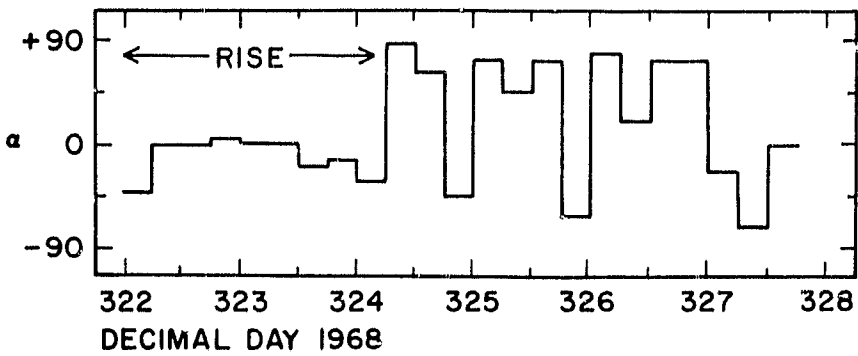
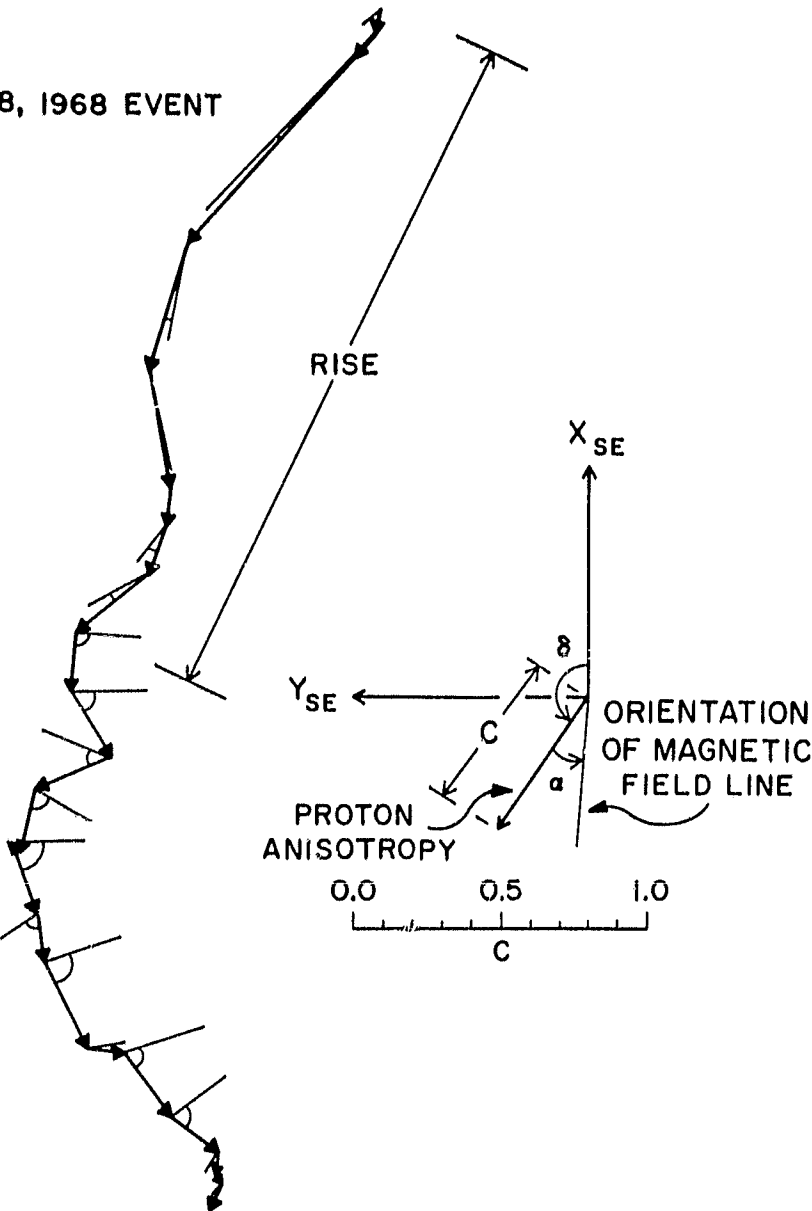


Figure 2



JANUARY 24, 1969 EVENT

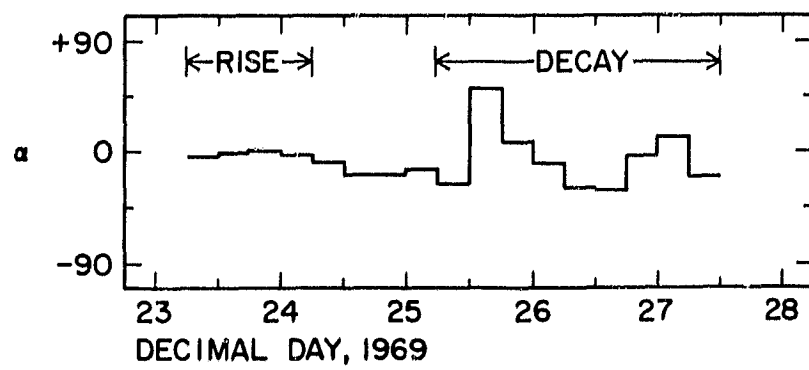
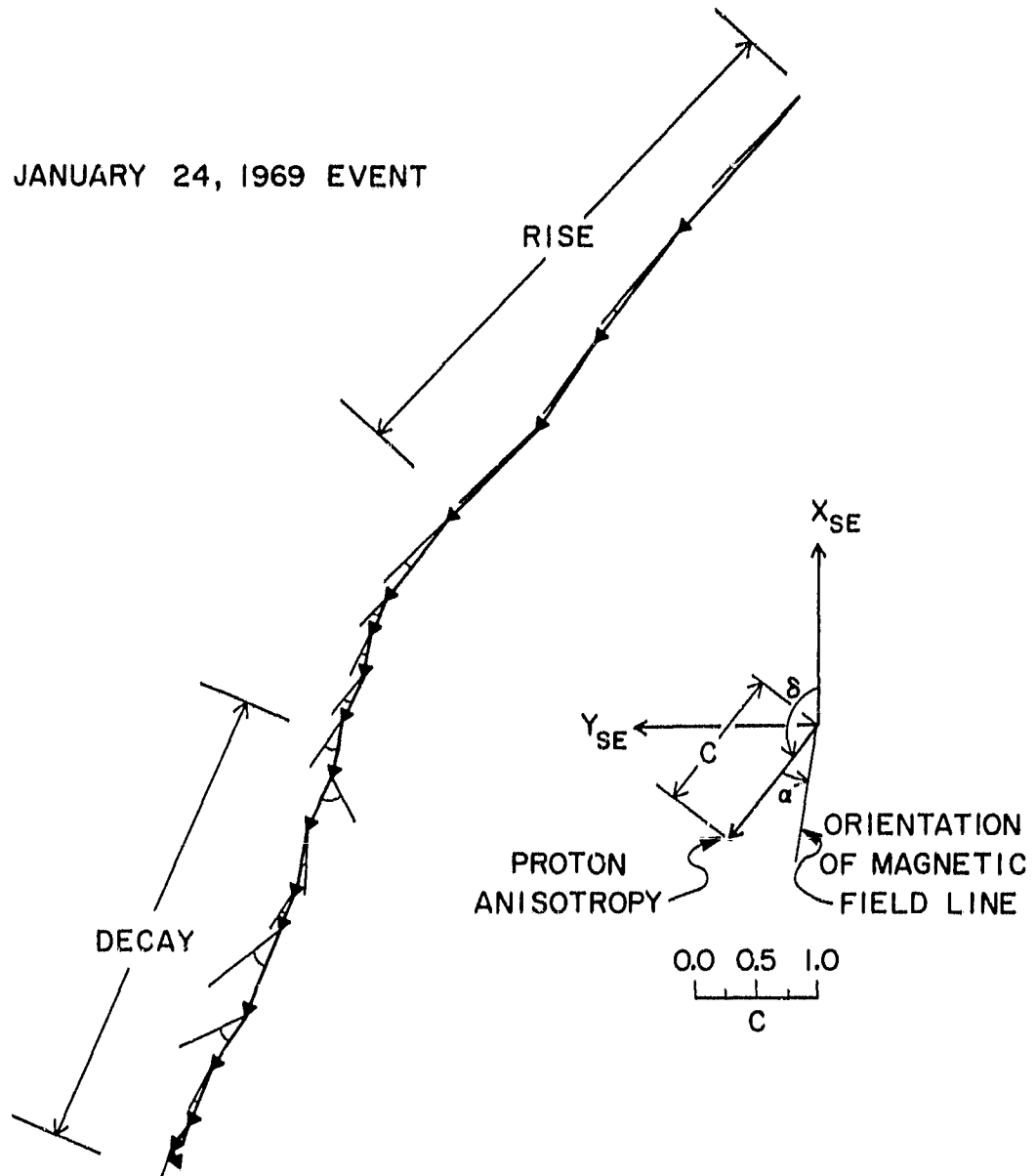


Figure 3

MARCH 21, 1969 EVENT

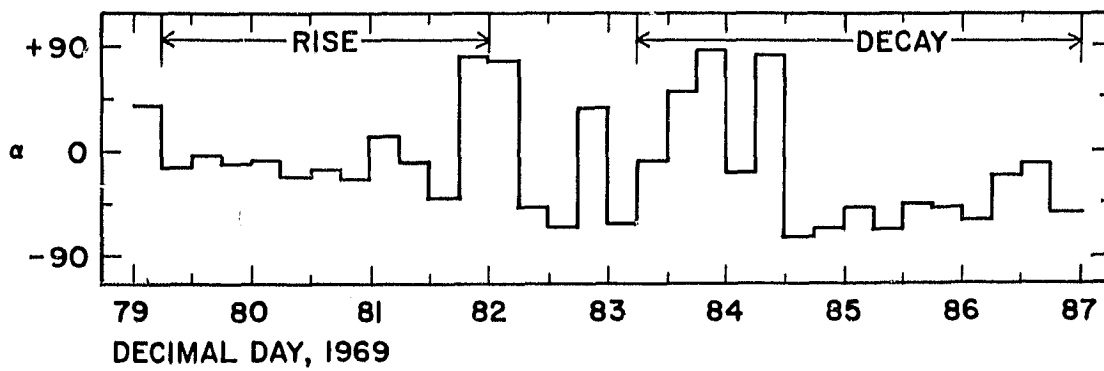
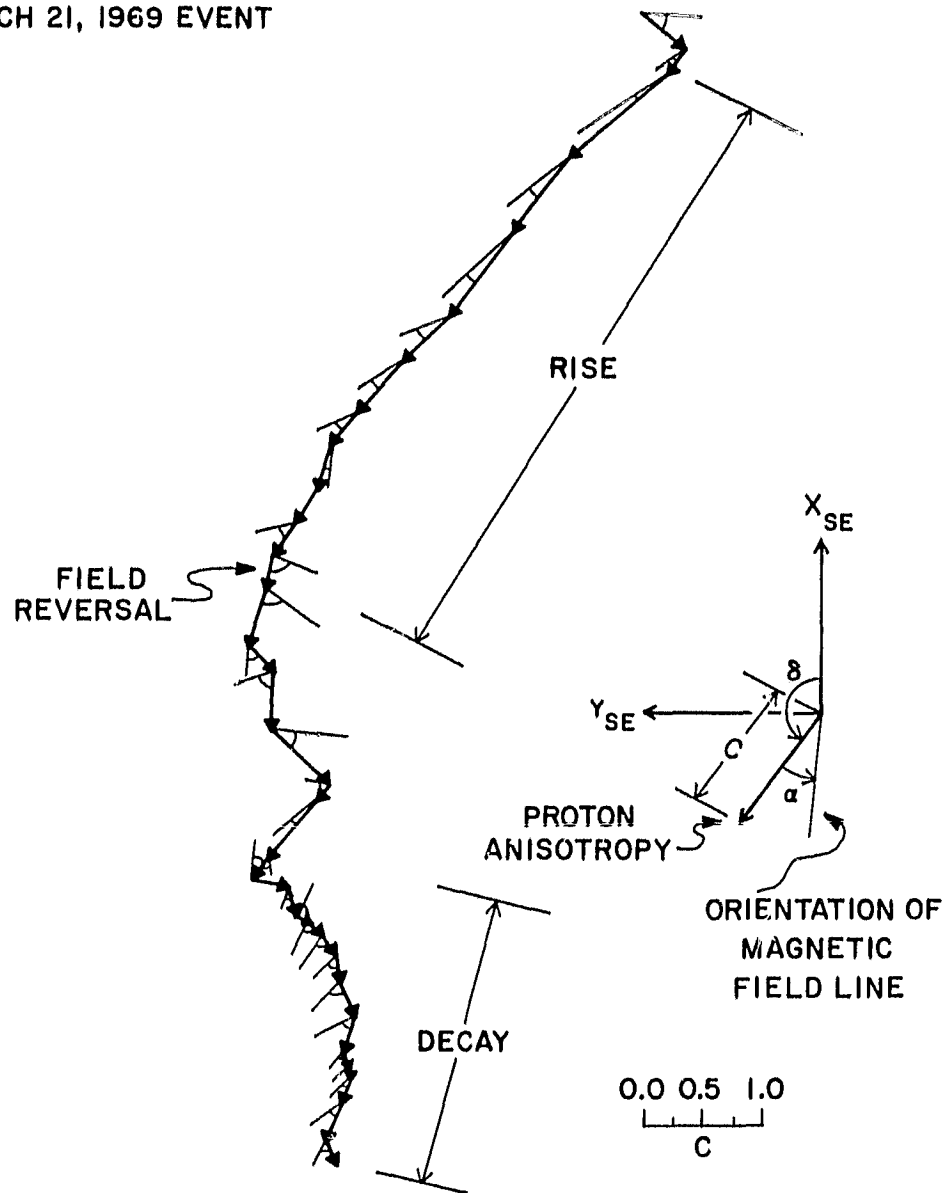


Figure 4

D-072-147

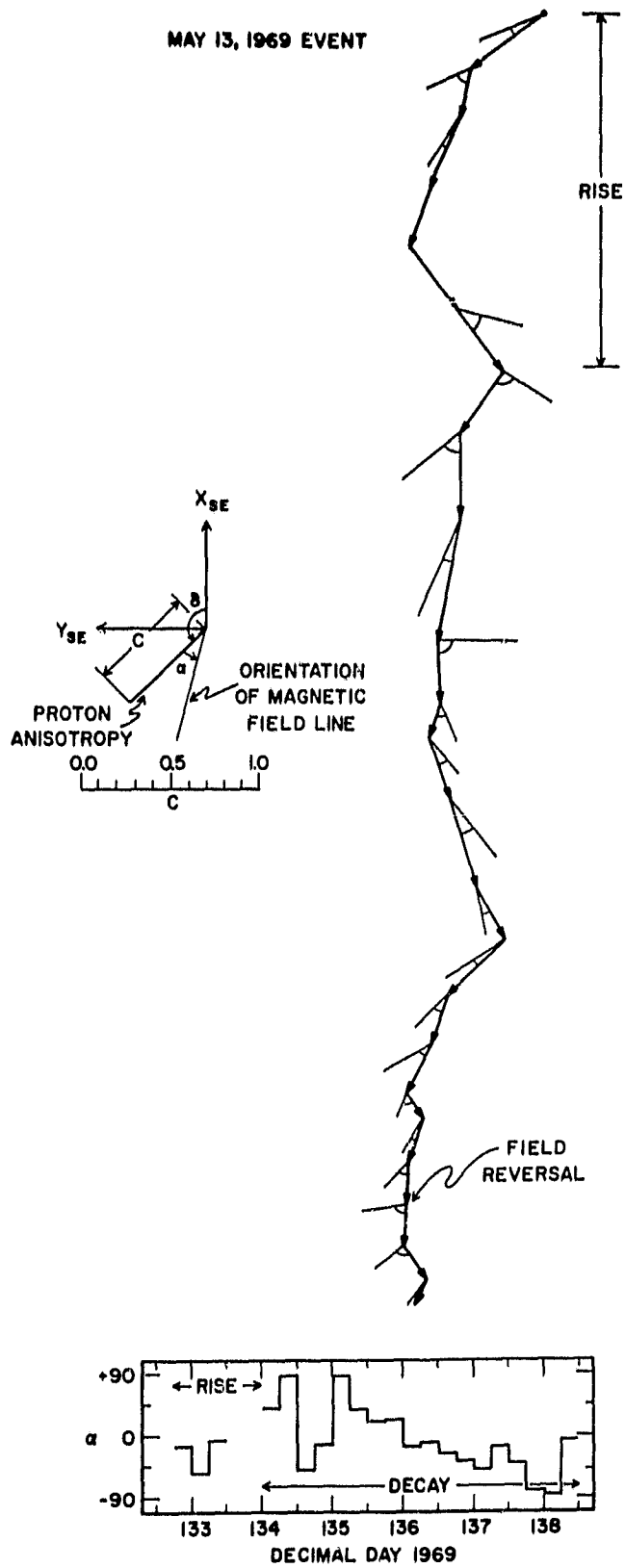


Figure 5

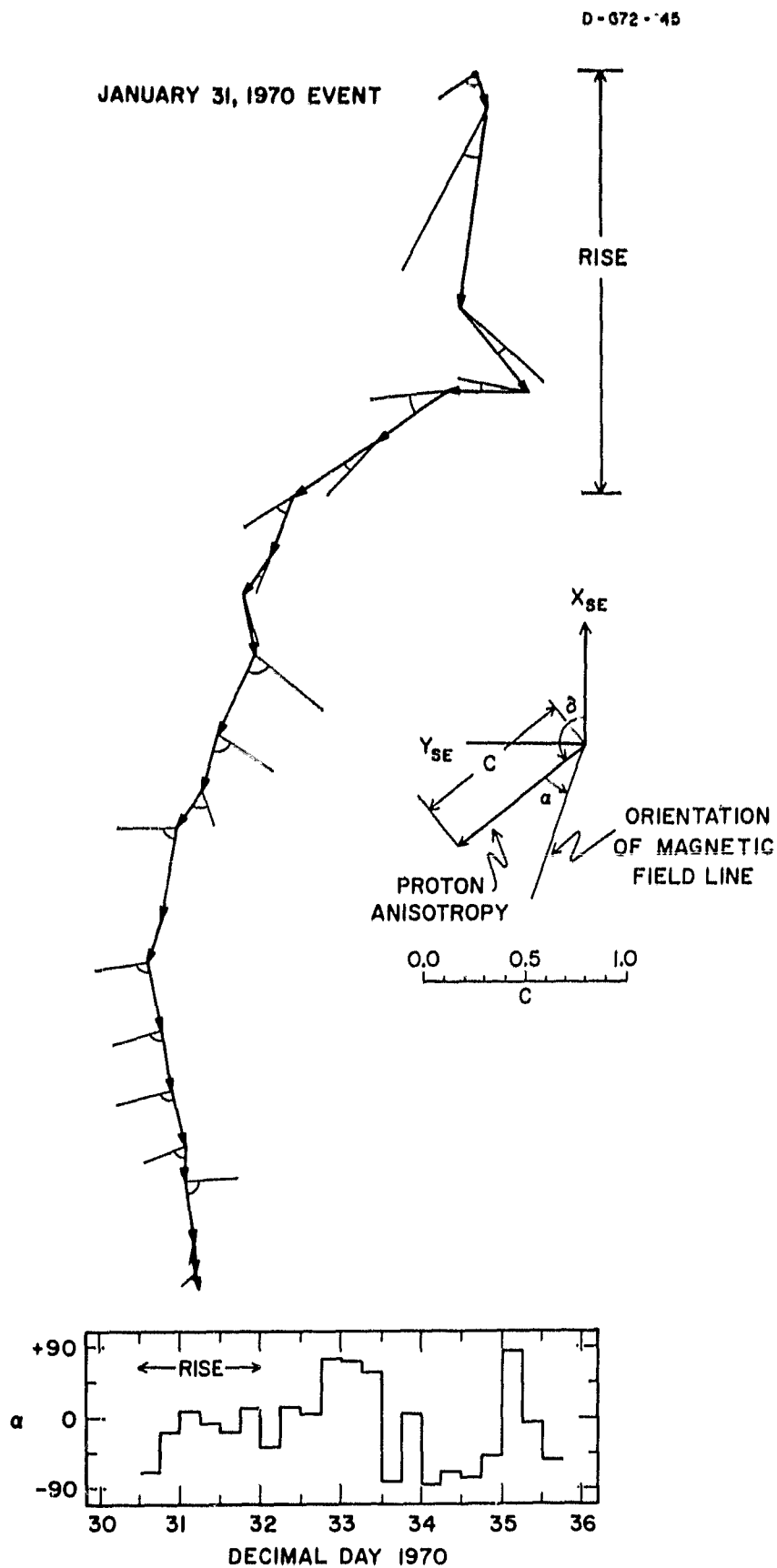


Figure 6

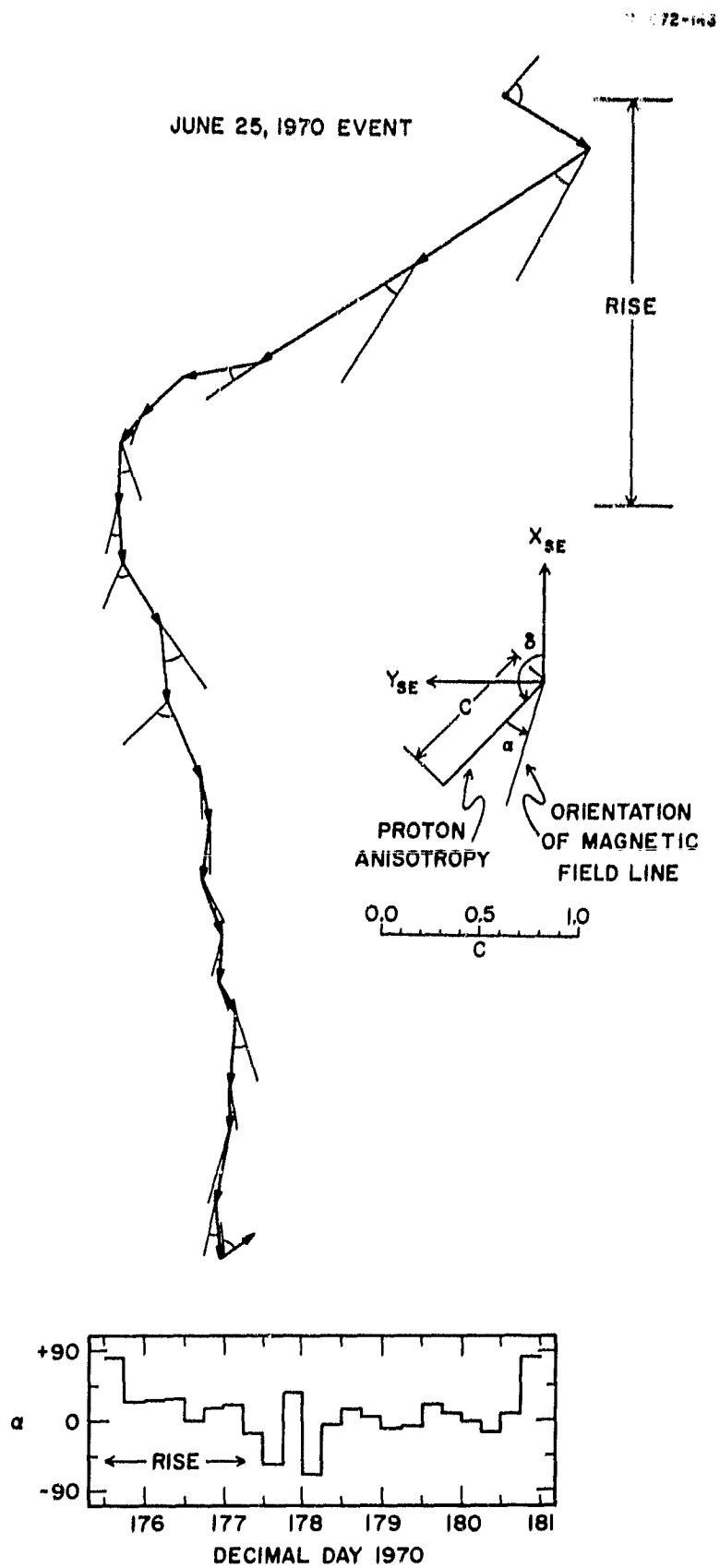


Figure 7

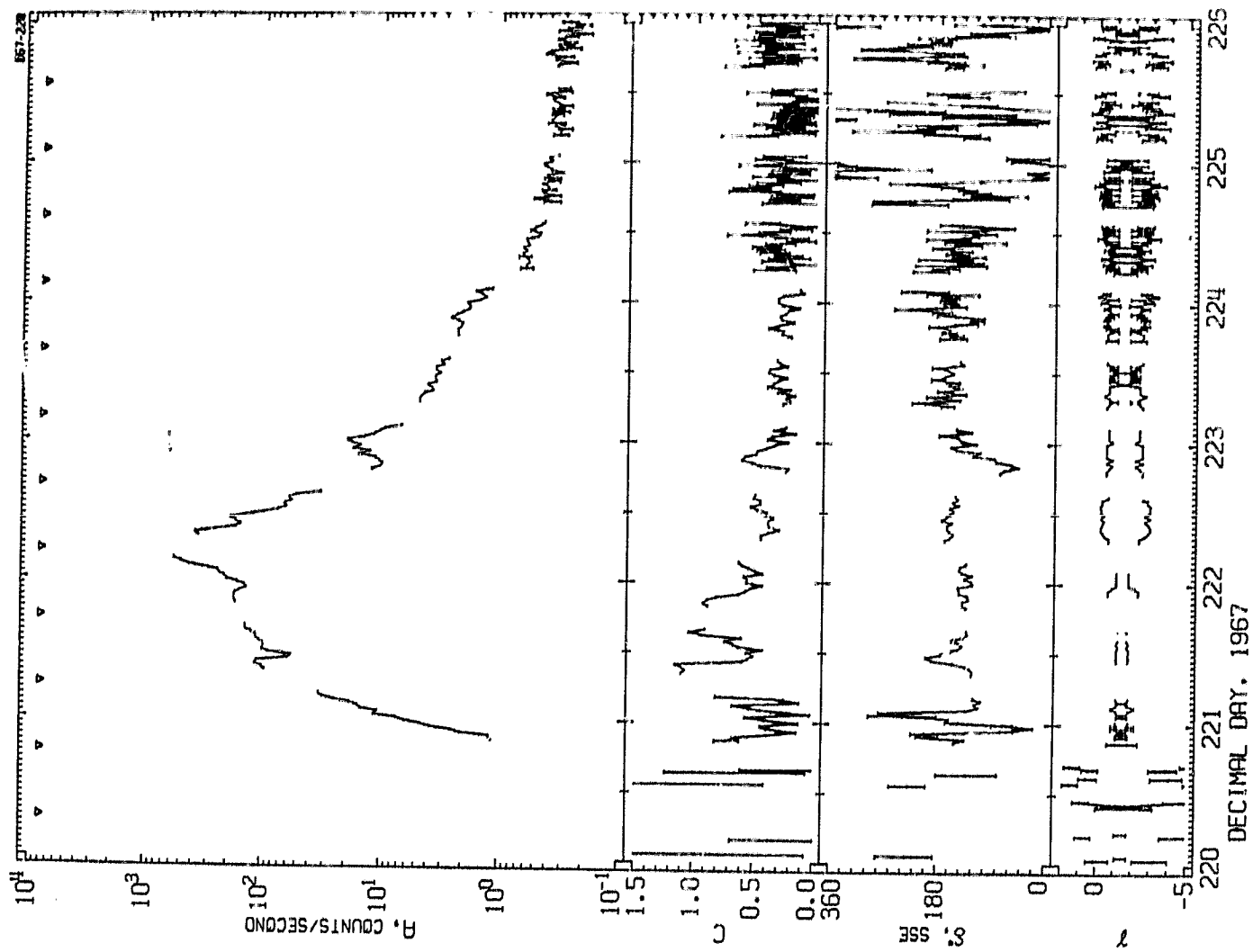


Figure 8

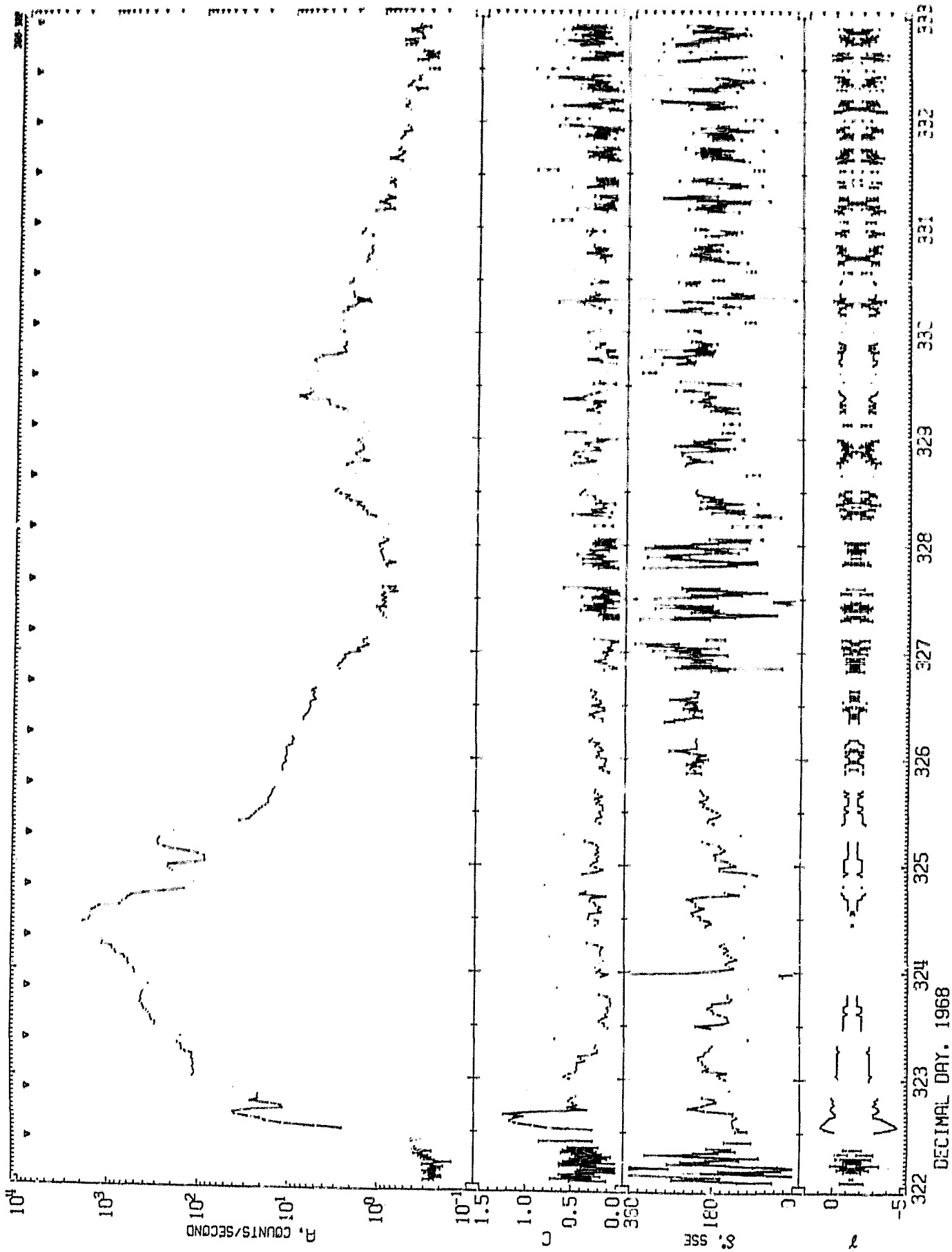


Figure 9

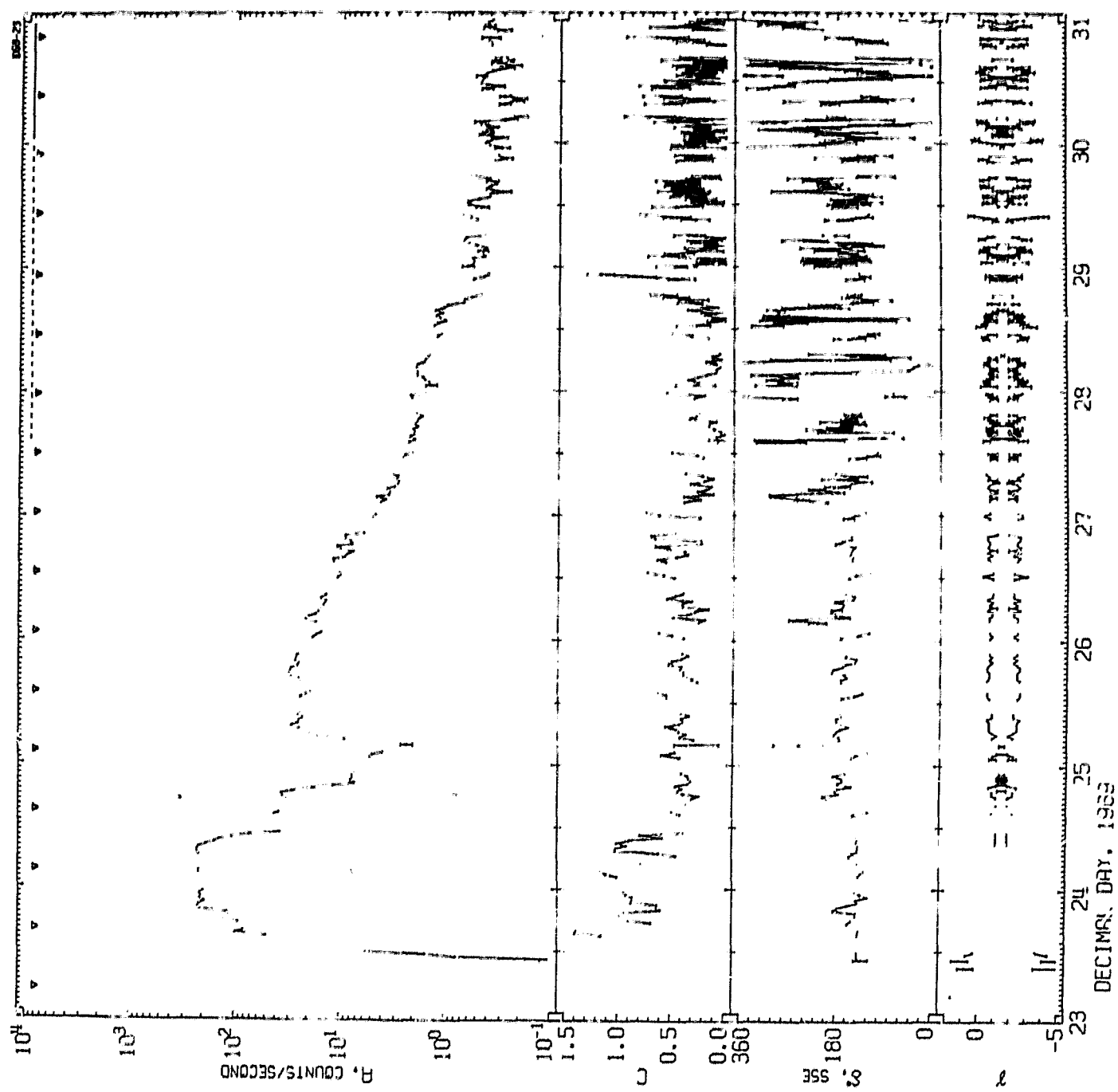


Figure 10



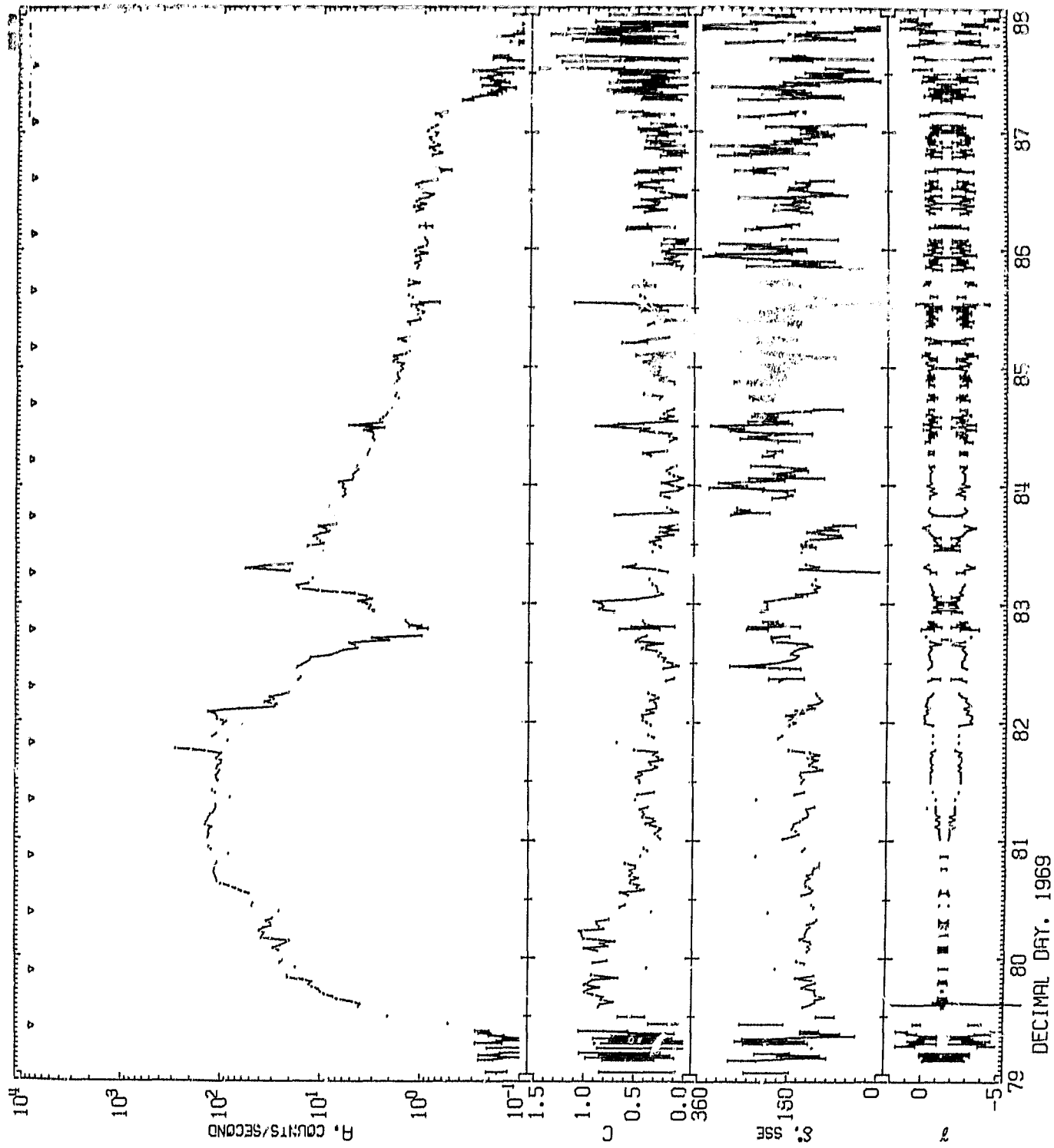


Figure 11

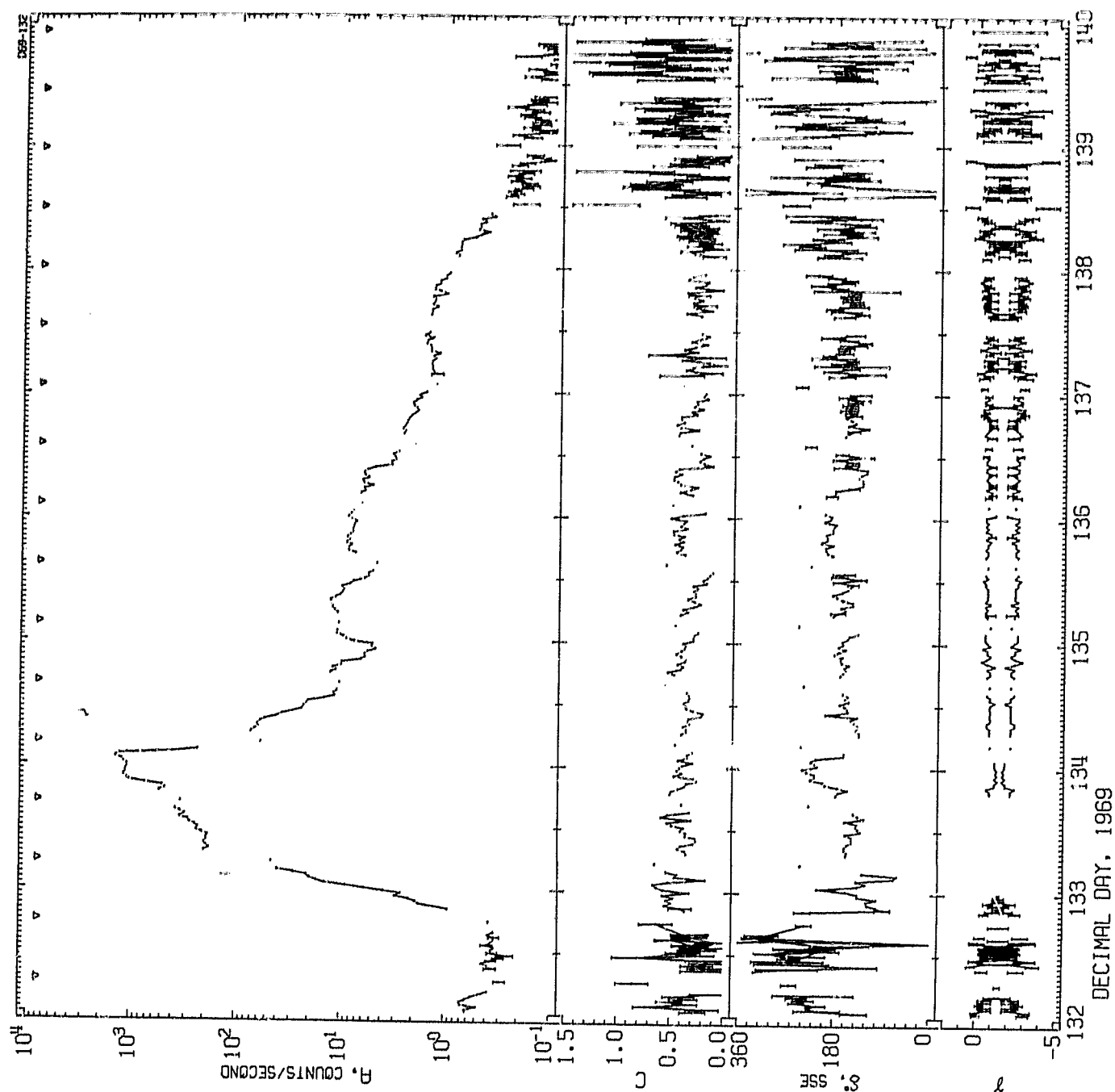


Figure 12

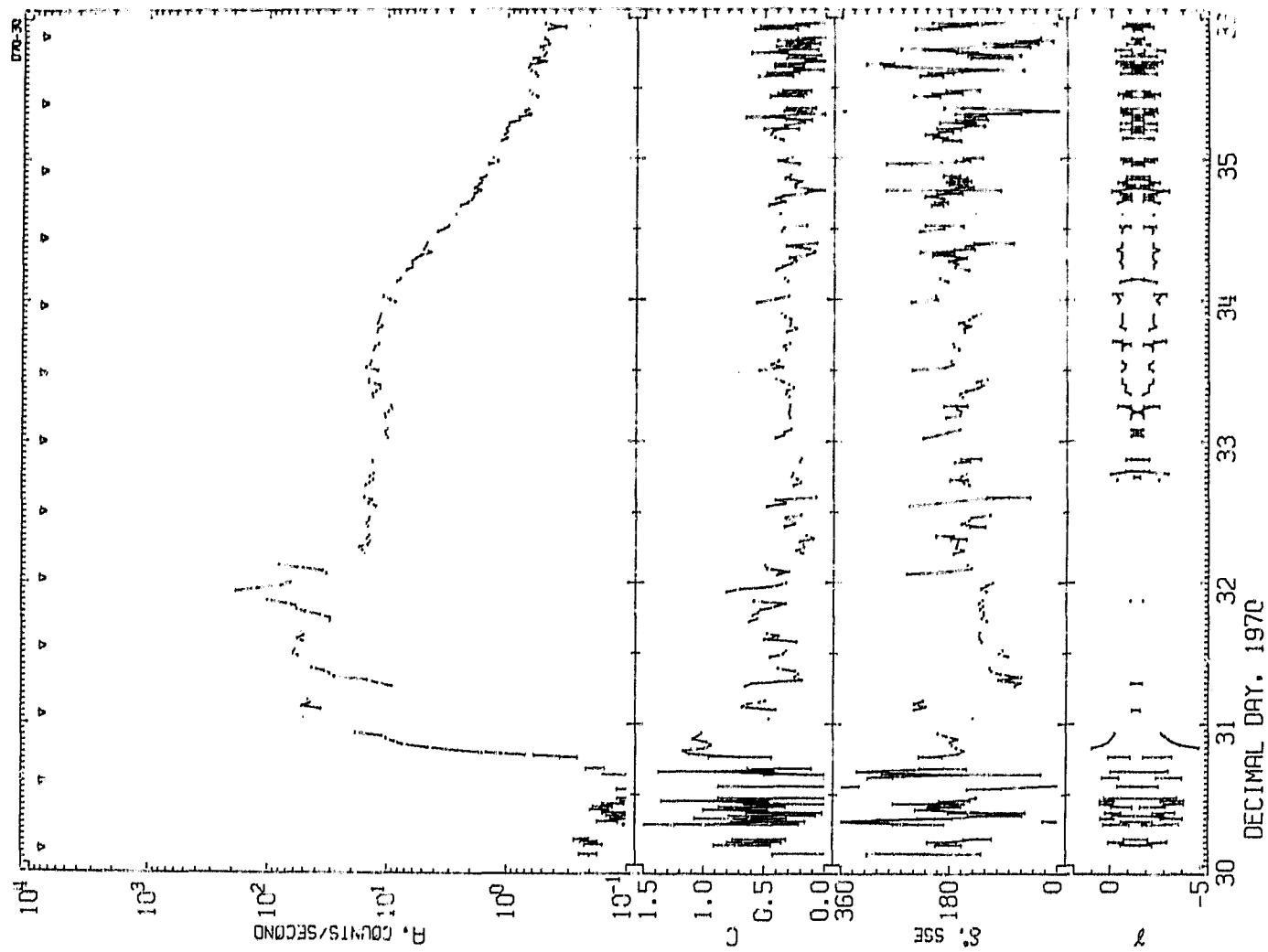


Figure 13

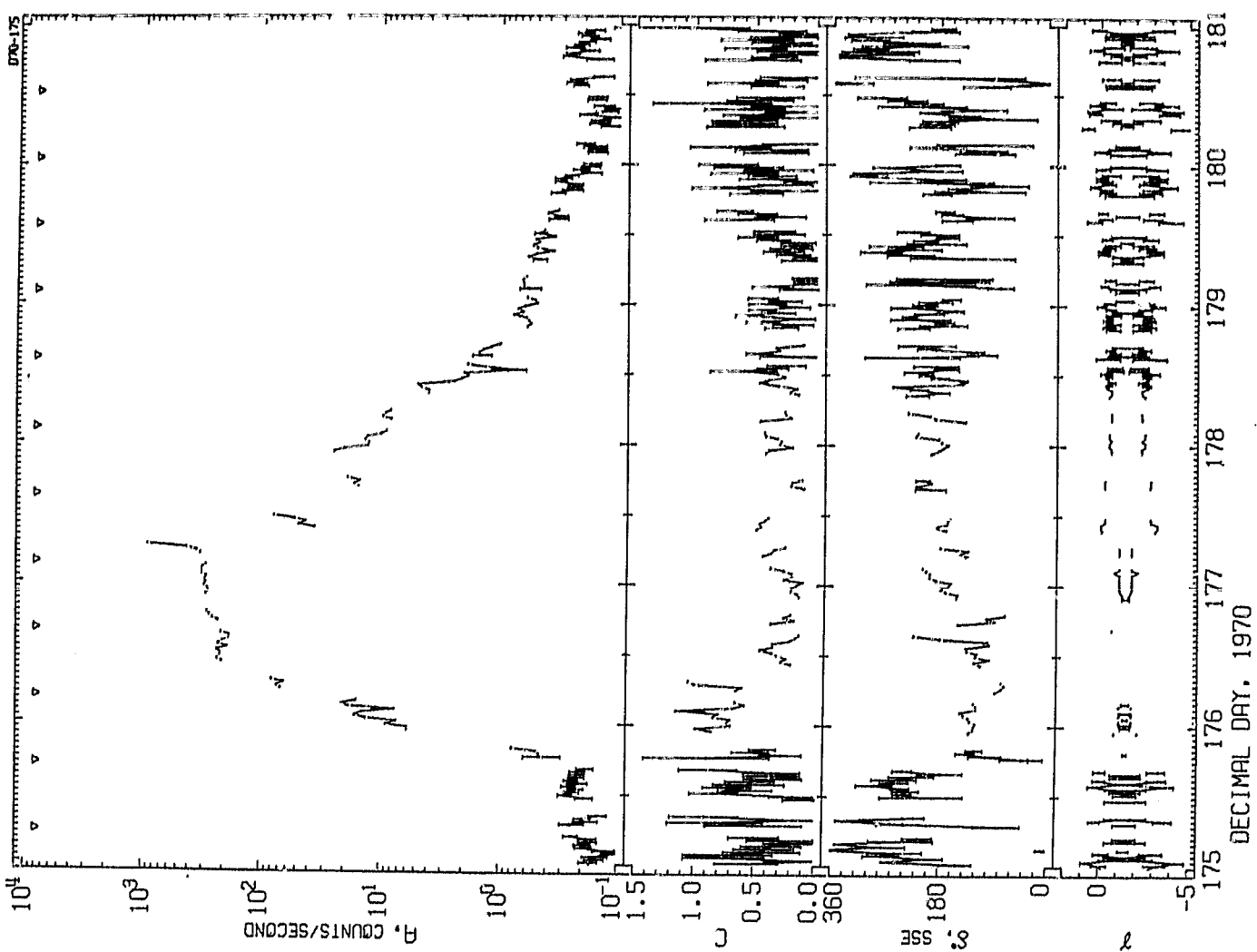


Figure 14

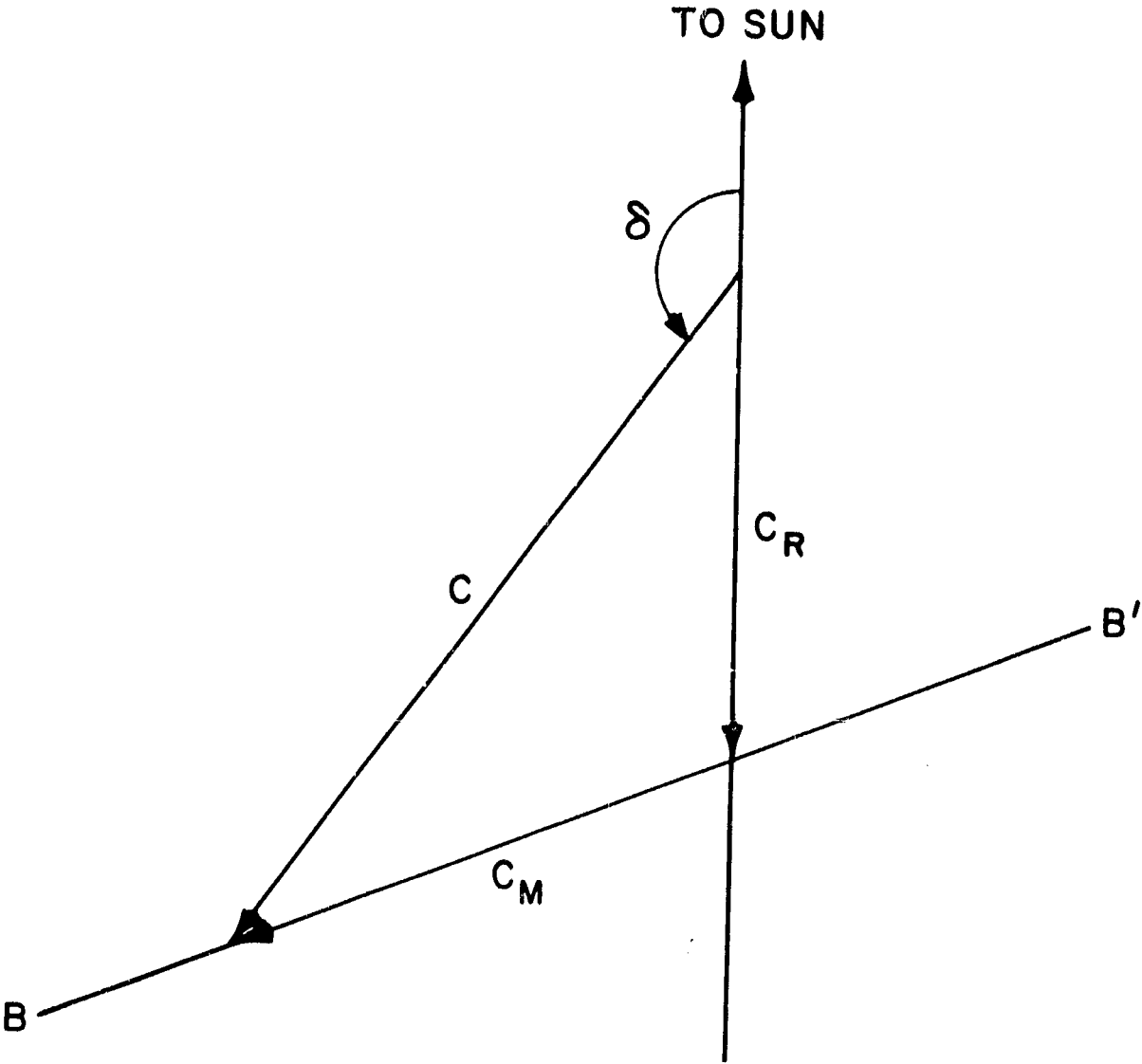


Figure 15

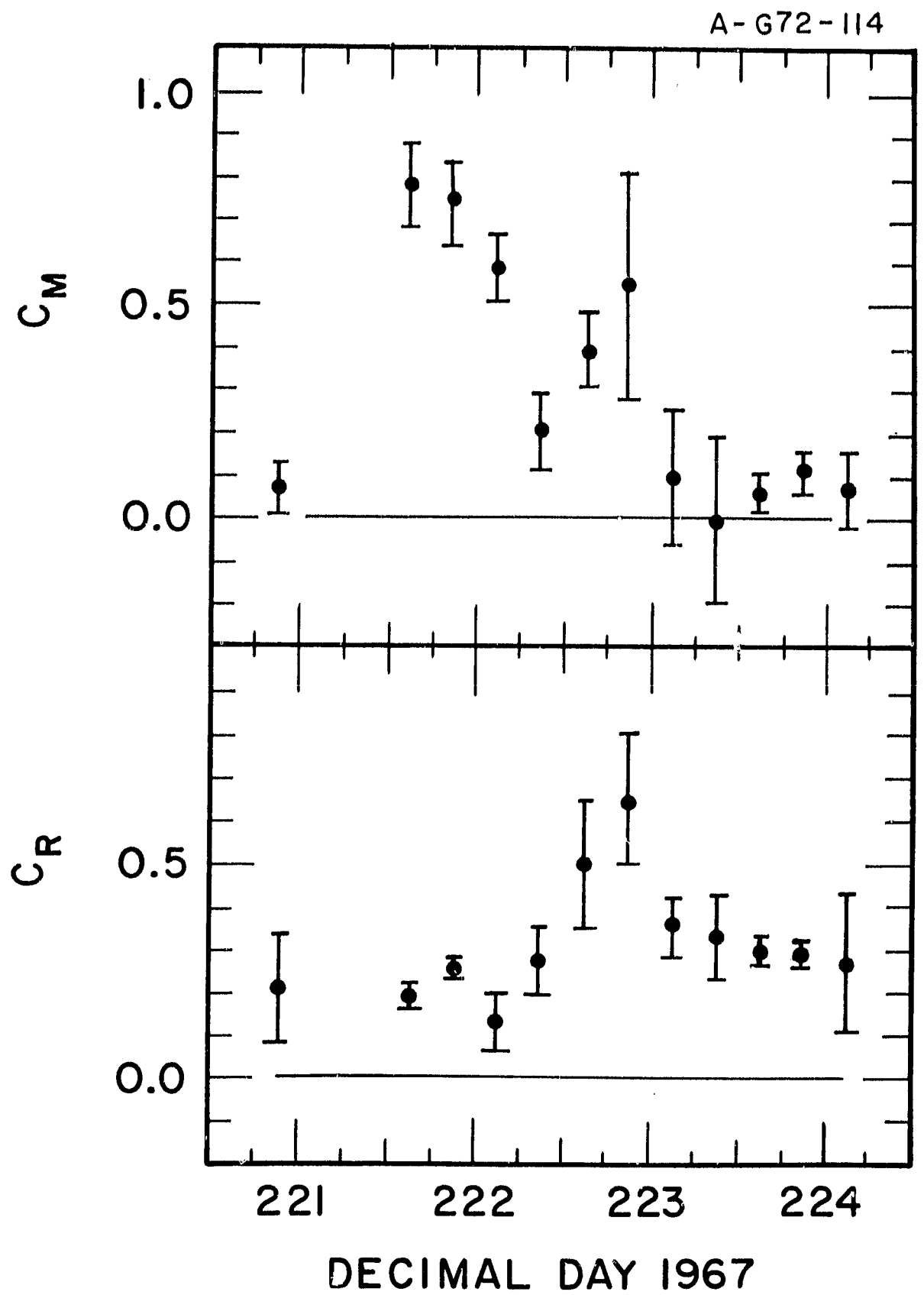


Figure 16

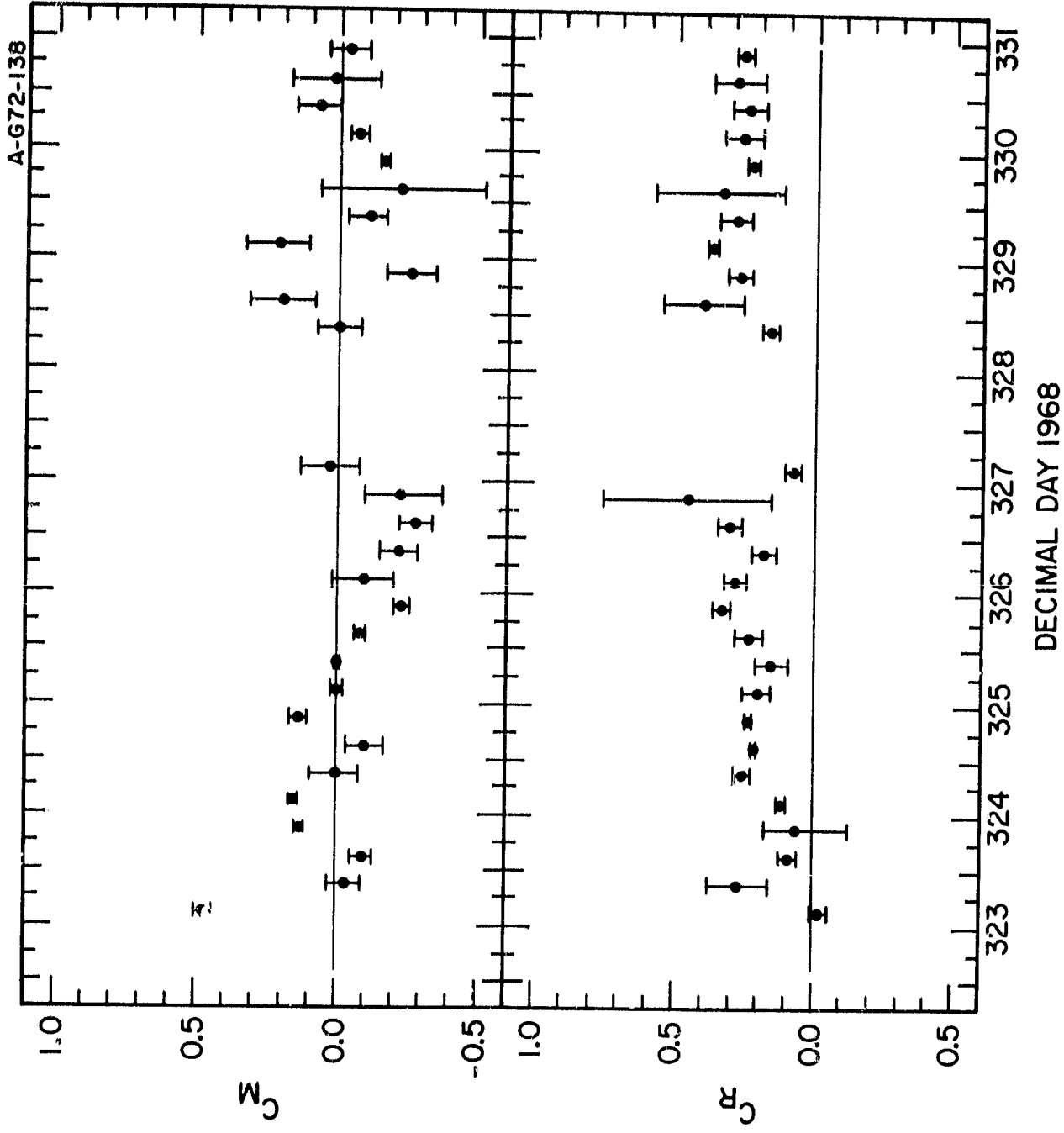


Figure 17

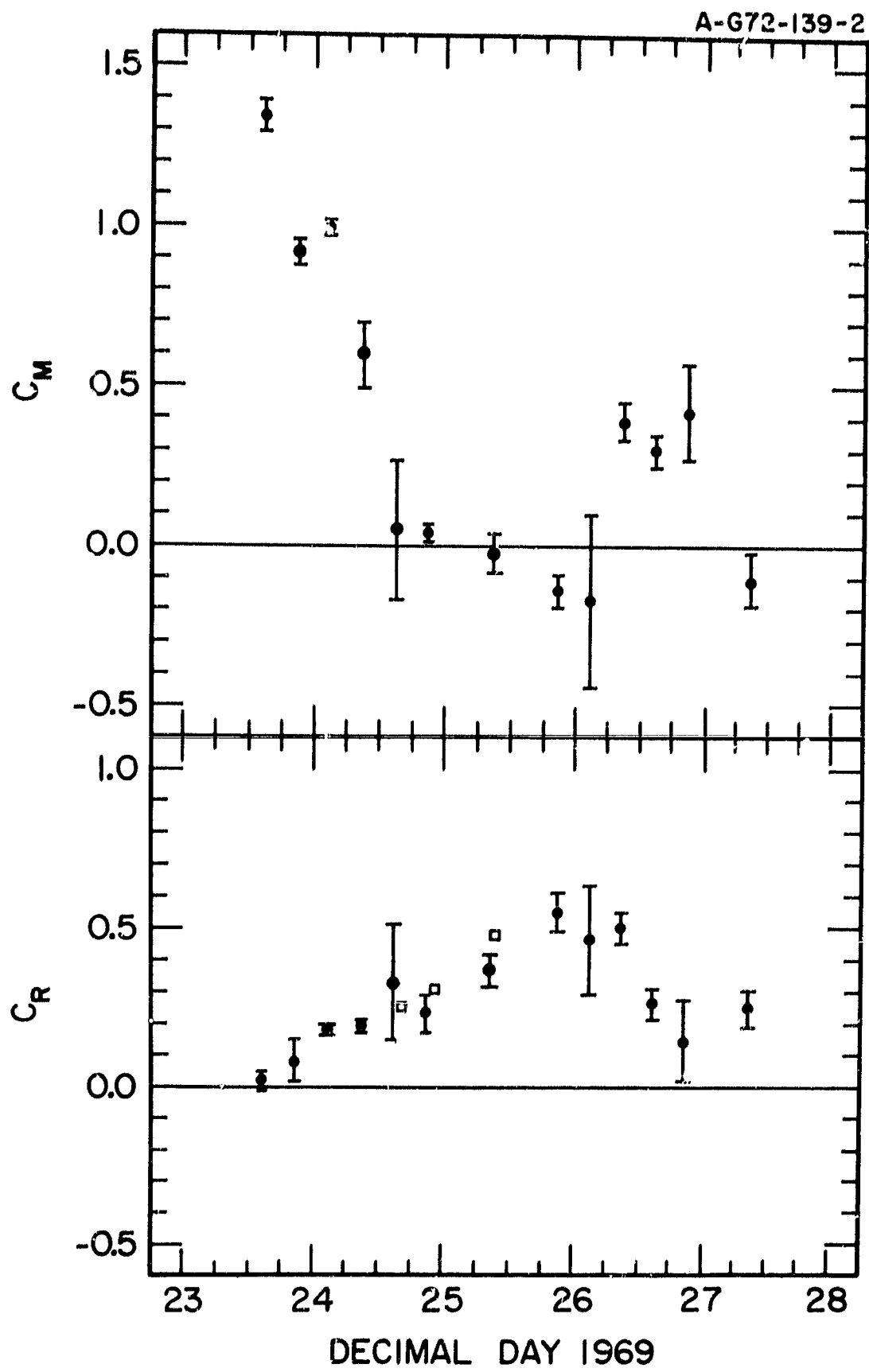


Figure 18



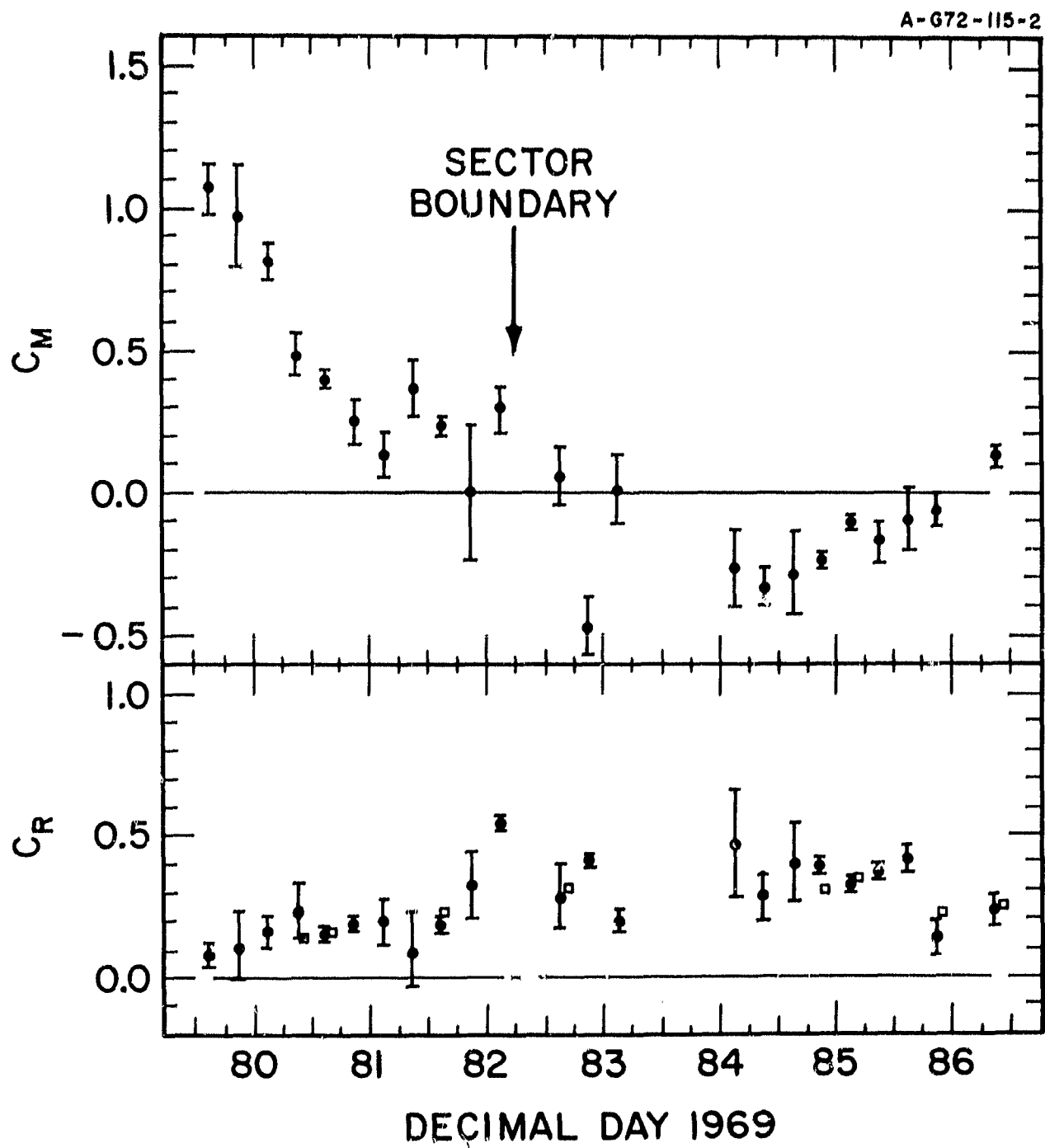


Figure 19

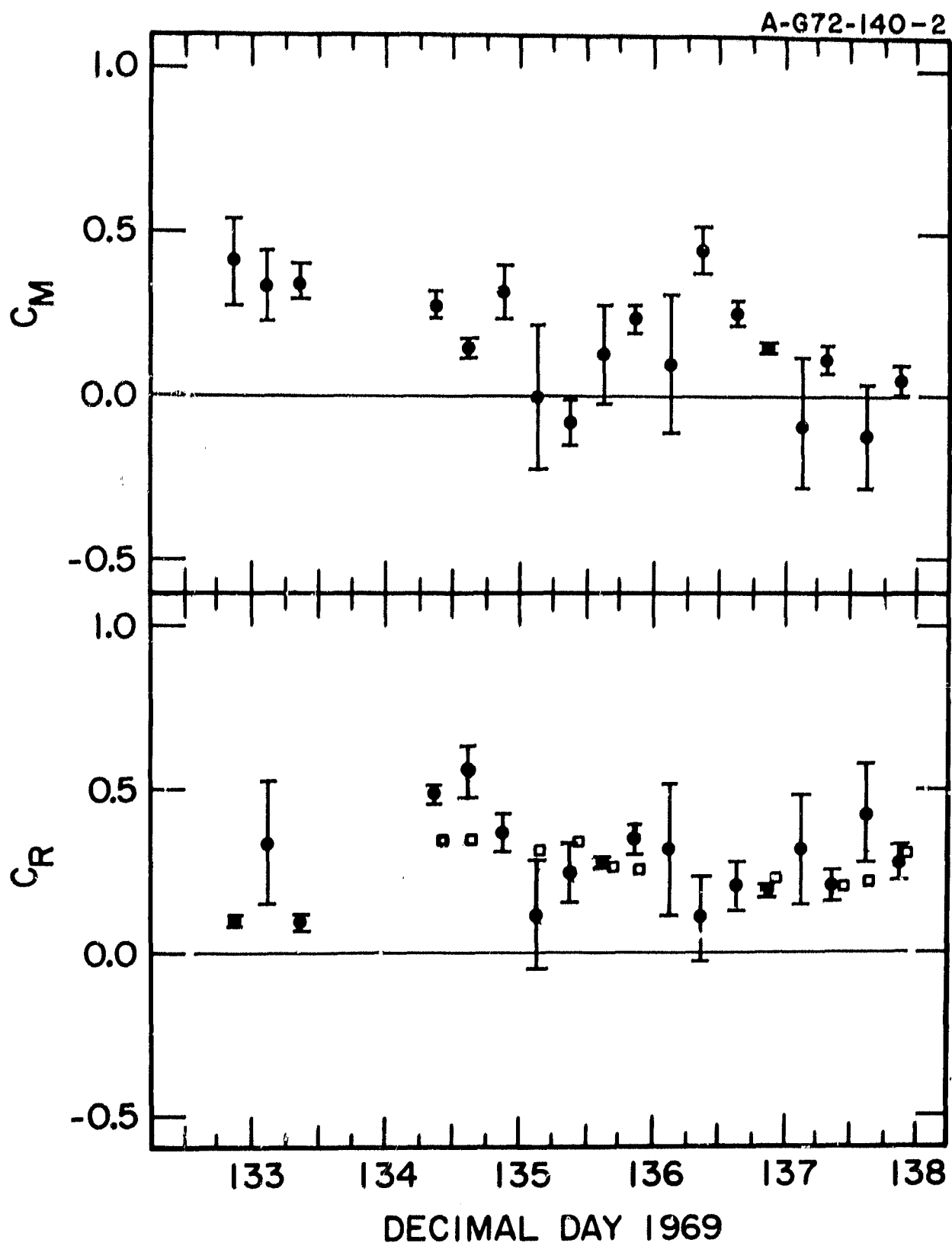


Figure 20

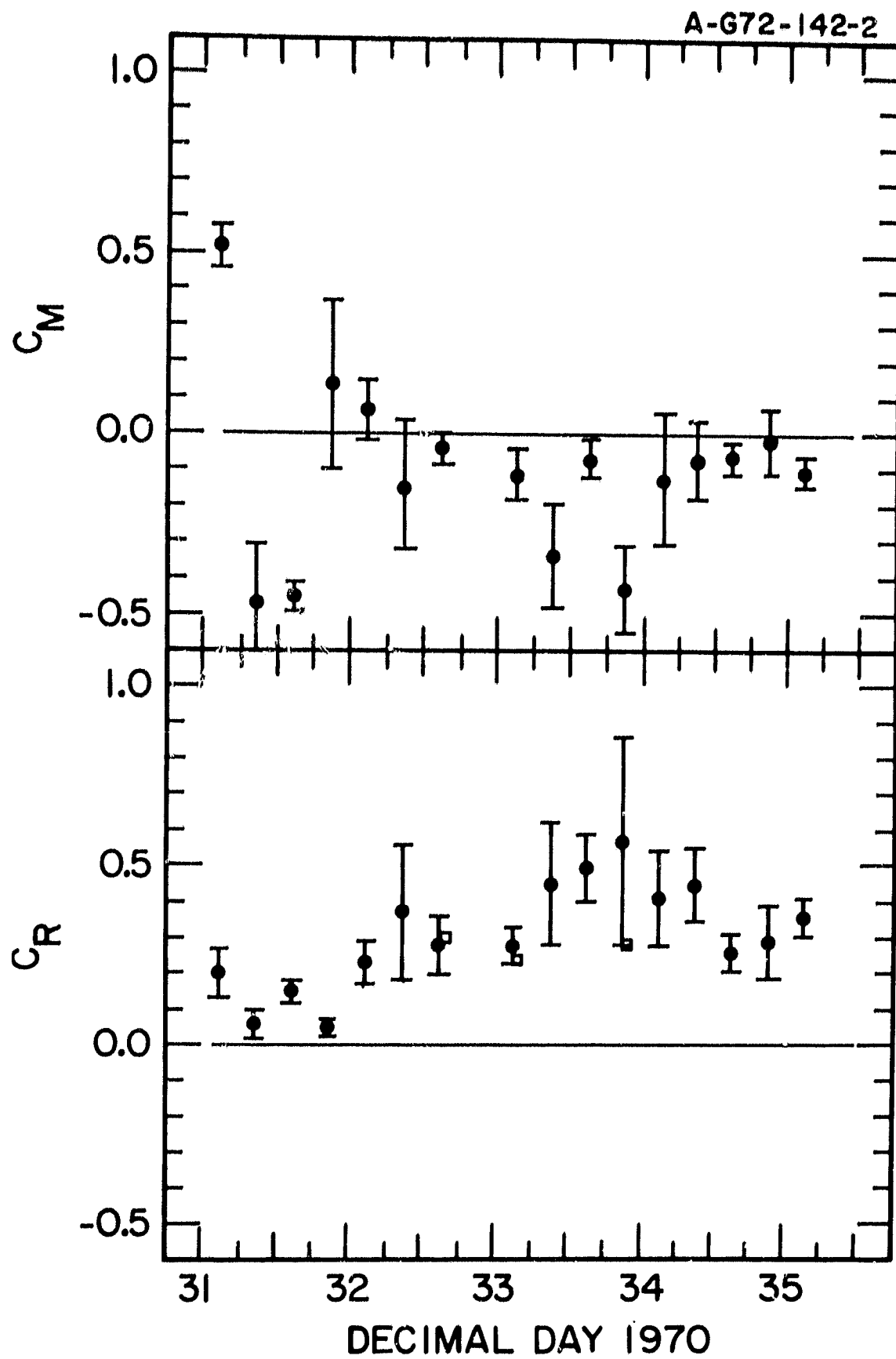


Figure 21

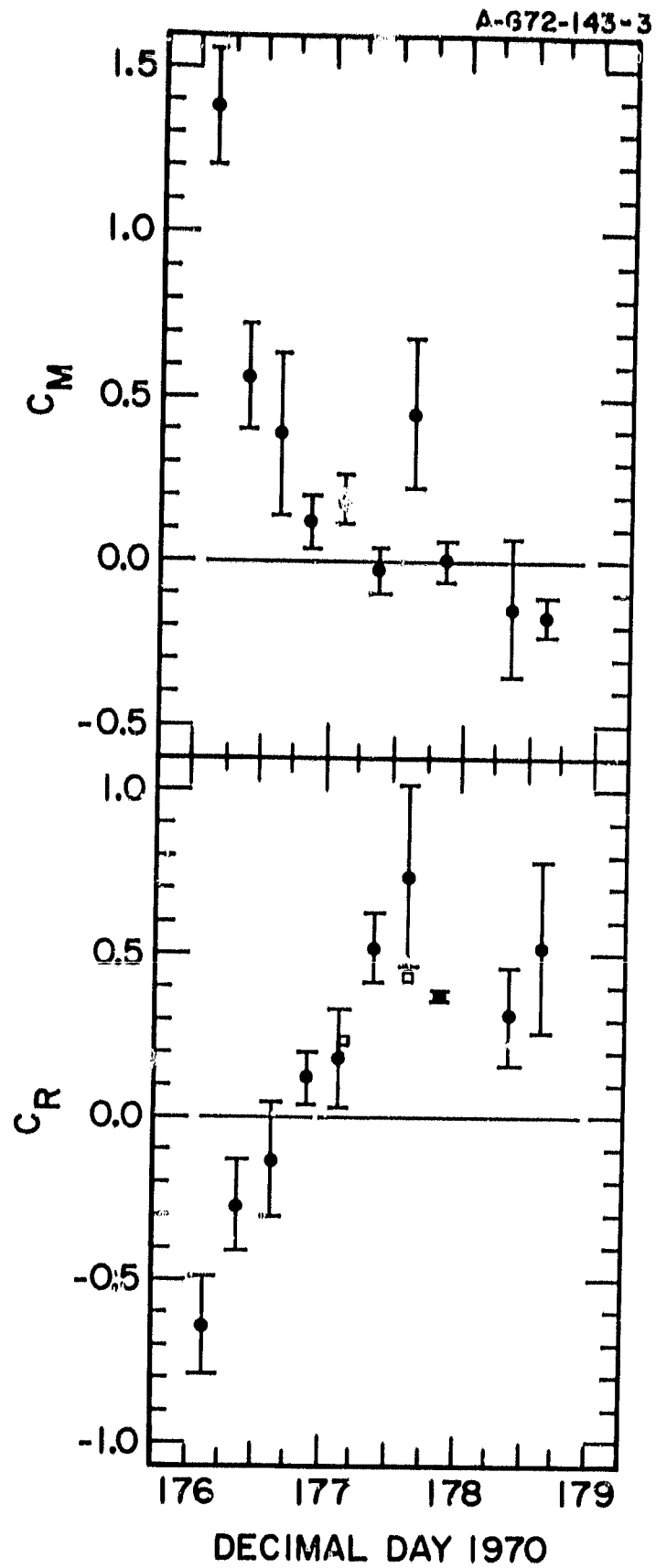


Figure 22

END